

NACA RM L52118

NOV 6 1952



# RESEARCH MEMORANDUM

LOW-SPEED STATIC LONGITUDINAL AND  
LATERAL STABILITY CHARACTERISTICS OF A MODEL WITH  
LEADING-EDGE CHORD-EXTENSIONS INCORPORATED ON A  
40° SWEEPBACK CIRCULAR-ARC WING OF ASPECT  
RATIO 4 AND TAPER RATIO 0.50

By Kenneth W. Goodson and Albert G. Few, Jr.  
CLASSIFICATION CHANGED

Langley Aeronautical Laboratory  
Langley Field, Va.

**FOR REFERENCE**

UNCLASSIFIED

By authority of NACA Res also effective Date June 24, 1958  
AMT 8-13-58 RN-128

NOT TO BE TAKEN FROM THIS ROOM

CLASSIFIED DOCUMENT

This material contains information affecting the National Defense of the United States within the meaning of the espionage laws, Title 18, U.S.C., Secs. 793 and 794, the transmission or revelation of which in any manner to unauthorized person is prohibited by law.

## NATIONAL ADVISORY COMMITTEE FOR AERONAUTICS

WASHINGTON  
November 3, 1952



3 1176 01436 9475

## NATIONAL ADVISORY COMMITTEE FOR AERONAUTICS

## RESEARCH MEMORANDUM

LOW-SPEED STATIC LONGITUDINAL AND  
LATERAL STABILITY CHARACTERISTICS OF A MODEL WITH  
LEADING-EDGE CHORD-EXTENSIONS INCORPORATED ON A  
40° SWEEPBACK CIRCULAR-ARC WING OF ASPECT  
RATIO 4 AND TAPER RATIO 0.50

By Kenneth W. Goodson and Albert G. Few, Jr.

## SUMMARY

An investigation was conducted to determine the aerodynamic effects at low speed of several wing leading-edge chord-extensions incorporated on a complete model having a 40° sweptback circular-arc wing of aspect ratio 4 and taper ratio 0.50. The tests indicate that the effectiveness of the chord-extension in increasing the stability is mainly dependent upon the spanwise inboard-end location of such a device. For a suitable inboard-end location (0.65 semispan from plane of symmetry for the present model) the chord-extension span could be changed from 35 to 15 percent wing semispan with little change in the stability or lift characteristics. Reduction of the chord-extension overhang from 15 to 10 percent of the local chord caused only a very slight decrease in the effectiveness of the device in improving the stability. With plain trailing-edge flaps retracted, the use of a leading-edge chord-extension appeared to be quite advantageous over a leading-edge fence located at the spanwise position (0.60 wing semispan) of the inboard end of the chord-extension. The fence provided essentially no increase in maximum lift and the pitching-moment curve suffered an unstable break at stall; whereas the chord-extension increased the maximum lift coefficient by about 23 percent and eliminated any serious loss in longitudinal stability throughout the lift range. By a suitable combination of a leading-edge chord-extension and deflection of a leading-edge flap, substantial improvements in drag due to lift and maximum lift coefficient could be obtained while maintaining favorable high-lift pitching-moment characteristics for plain trailing-edge flaps either neutral or deflected. For such a configuration, however, it was essential that the leading-edge flaps include the chord-extension and extend an appreciable distance inboard from the chord-extension.

The use of chord-extensions for the flaps-neutral configuration increased the effective dihedral in the moderate- to high-lift-coefficient range, but did not appreciably alter the directional stability characteristics.

## INTRODUCTION

The use of swept wings with thin airfoil sections offers promising solutions to some of the aerodynamic problems encountered in high-speed flight. However, wings of this type generally exhibit a type of flow separation characterized by a vortex that lies above the surface near the leading edge, and, for some plan forms, this flow can cause undesirable changes in longitudinal stability at moderate and high lift coefficients. Previous investigations at low speeds have shown that these undesirable characteristics can be alleviated by the use of wing leading-edge chord-extensions, fences, or trailing-edge extensions (refs. 1 to 4). The chord-extensions appear to change the spanwise loading such that the nose-up tendency at high lift coefficients is reduced. As was pointed out in reference 2 such devices could be extended when required, or if the high-speed characteristics proved satisfactory, they could be fixed.

The tests reported herein were made with a complete model that incorporated a  $40^\circ$  sweptback (quarter-chord line), 10-percent-thick circular-arc wing of aspect ratio 4 and taper ratio 0.50. The present paper presents low-speed aerodynamic characteristics of a typical airplane model without and with chord-extensions located at various spanwise positions on the outboard portion of the wing for various flap arrangements. These data include comparisons of characteristics for various chord-extension spans having an optimum inboard-end location. Data were obtained to determine the effect of deflecting the wing leading edge with a chord-extension having an optimum inboard-end location. A comparison of the longitudinal stability characteristics was also made when the wing was equipped with a fence. Lateral stability parameters are presented for both clean-wing and chord-extension configurations with the plain trailing-edge flaps retracted.

## SYMBOLS

The system of axes employed, together with an indication of the positive directions of forces, moments, and angles is shown in figure 1. The aerodynamic force and moment coefficients are based on the clean-wing area unless otherwise noted on the figures. All pitching-moment coefficients are presented about the quarter-chord point of the clean-wing mean aerodynamic chord. The symbols used herein are defined as follows:

$C_L$	lift coefficient, $\frac{\text{Lift}}{qS}$
$C_X$	longitudinal-force coefficient, $\frac{X}{qS}$
$C_Y$	lateral-force coefficient, $\frac{Y}{qS}$
$C_l$	rolling-moment coefficient, $\frac{L}{qSb}$
$C_m$	pitching-moment coefficient, $\frac{M}{qSc}$
$C_n$	yawing-moment coefficient, $\frac{N}{qSb}$
X	longitudinal force along X-axis, Drag = -X, lb
Y	lateral force along Y-axis, lb
Z	force along Z-axis, Lift = -Z, lb
L	rolling moment about X-axis, ft-lb
M	pitching moment about Y-axis, ft-lb
N	yawing moment about Z-axis, ft-lb
q	free-stream dynamic pressure, $\frac{\rho V^2}{2}$ , lb/sq ft
$q_t$	effective dynamic pressure at the tail, lb/sq ft
$\epsilon$	effective downwash angle at tail, deg
S	clean-wing area, sq ft
$\bar{c}$	clean-wing mean aerodynamic chord, ft
c	local wing chord perpendicular to the 50-percent-chord line, ft
c'	local wing chord parallel to plane of symmetry, ft
b	wing span, ft
V	free-stream velocity, ft/sec

$\rho$	mass density of air, slugs/cu ft
$\alpha$	angle of attack with respect to fuselage center line, deg
$\beta$	angle of sideslip, deg
$i_t$	angle of incidence of stabilizer with respect to fuselage center line, deg
$\delta_f$	plain trailing-edge flap deflection, perpendicular to 0.50 chord line, deg
$\delta_n$	wing leading-edge flap deflection, perpendicular to 0.50-chord line, deg

Subscripts:

$\beta, \alpha$	denotes partial derivative of a coefficient with respect to sideslip or angle of attack (for example, $C_{L\beta} = \frac{\partial C_L}{\partial \beta}$ , $C_{L\alpha} = \frac{\partial C_L}{\partial \alpha}$ )
t	contributed by horizontal tail
n	wing nose flap
1, 2, 3	denote portions of wing leading-edge flaps deflected

#### DESCRIPTION OF MODEL

The general arrangement of the model used in this investigation is given as figure 2 with other characteristics being presented in table I. The model wing had a  $40^\circ$  sweptback quarter-chord line, aspect ratio 4, taper ratio 0.50, and incorporated a 10-percent-thick circular-arc airfoil section normal to the 50-percent-chord line. The model had 0.20c plain trailing-edge flaps, which extended over 50 percent of the wing span from the plane of symmetry. Figure 3 shows details of the 0.15c leading-edge flaps (hinge line in chord plane) of which various spanwise elements could be deflected. Details of chord-extensions extending from the wing tip to various inboard spanwise stations are shown in figure 4, whereas figure 5 gives details of a series of chord-extensions running various distances outward from the 0.65b/2 station. Most of the tests were made with a chord-extension overhang of 0.15c, although some limited tests were made with 0.10c overhang. Details of a wing fence configuration are given in figure 6. Photographs of the model on the single

support strut are shown as figure 7. The model was constructed of wood and finished with several coats of lacquer.

### TESTS

A series of chord-extensions were tested on a model in the Langley 300 MPH 7- by 10-foot wind tunnel for various flap configurations with and without a horizontal tail. Longitudinal forces and moments were measured through an angle-of-attack range up to about  $19^{\circ}$ . A few additional tests were made through the angle-of-attack range of  $15^{\circ}$  sideslip to obtain lateral-stability parameters. Effective downwash and dynamic pressures at the tail were determined from the pitching-moment data.

The flaps-neutral tests were made at a dynamic pressure of 41 pounds per square foot, which corresponds to a Mach number of 0.17 and to a Reynolds number of  $2.2 \times 10^6$  based on the mean aerodynamic chord of the clean-wing configuration for average test conditions. Tests with flaps deflected were made at a dynamic pressure of 22 pounds per square foot, which corresponds to a Mach number of 0.12 and to a Reynolds number of  $1.62 \times 10^6$ .

### CORRECTIONS

No attempt was made to determine tare corrections resulting from the support strut. Except for effects on drag, it is believed that the tares are negligible.

The angle of attack, drag, and pitching-moment results have been corrected for jet-boundary effects computed on the basis of unswept-wing theory by the methods of reference 5. Vertical buoyancy on the support strut, longitudinal-pressure gradient, and tunnel air-flow misalignment have been accounted for in computation of the test data. All coefficients have been corrected for blocking by a method given in reference 6.

### RESULTS AND DISCUSSION

#### Presentation of Results

Results of exploratory tests to establish desirable chord-extension geometry on the basis of effects on static longitudinal stability

characteristics of the test model are presented in figures 8 to 11. Figures 12 and 13 present the effects of wing chord-extensions in conjunction with leading-edge flaps with plain trailing-edge flaps neutral and deflected. Stabilizer tests of the model with two of the better chord-extension arrangements are shown in figures 14 to 16 for various flap deflections. The effects of the chord-extensions on the effective downwash, on  $q_t/q$ , and on some of the significant longitudinal aerodynamic parameters are shown in figures 17 to 20. The effects of chord-extensions on the lateral-stability parameters are given in figure 21.

### General Remarks

The use of leading-edge chord-extensions has appeared quite promising as one of the various means of alleviating the tendency toward longitudinal instability at high lift coefficients, such as has been exhibited by many airplanes having sweptback wings. The action of these devices, as indicated by tuft studies on and near the wing surface, wake surveys, and the analysis of force-test data, has been described in references 2 to 4. The result of the chord-extension appears to be a change in spanwise loading such that the nose-up tendency at high lift coefficients normally is reduced. In general, the change in span loading results in an effect on the wing pitching-moment characteristics or an additional effect on the tail contribution to pitching moment caused by a change in the downwash or dynamic-pressure characteristics at the tail or both effects. The degree of change in spanwise loading is mainly dependent upon the inboard-end location of the chord-extension. These characteristics are evident in the present results.

### Static Longitudinal Characteristics

Effects of inboard-end location of chord-extensions.- Results of the investigation to determine the optimum inboard-end location of the 0.15c wing leading-edge chord-extensions on the present complete model are given in figure 8. For the clean-wing configuration (fig. 8), undesirable changes in stability are noticeable at lift coefficients well below stall (at about  $C_L = 0.6$ ). The data obtained with chord-extensions having various inboard-end locations indicate that all the arrangements tested provide improved stability characteristics from moderate to high lifts; however, the most desirable inboard-end location appears to be at about the 60- to 65-percent semispan station. Addition of the chord-extensions for the flaps-neutral configuration is seen to cause only small changes in the effective downwash angles at the tail (fig. 17), although some reduction in dynamic-pressure ratio is experienced (fig. 18). The net result on tail pitching moments is small for

the flaps-neutral configuration as is shown in figure 19. For the present model, therefore, the improvement in stability characteristics is primarily a result of the direct effect on the wing, as is also shown by the data of figure 14. The probable reason for the small downwash change resulting from the addition of chord-extensions is that the horizontal-tail span of the model investigated is largely inboard of the influence of the shed vortices, except possibly at angles of attack near the stall. The presence of these vortices was observed on a tuft grid located behind the model.

The results given in figure 8 show that a considerable increase in maximum lift coefficient ( $\Delta C_{l_{max}} = 0.13$  to  $0.20$ ) is obtained by the addition of wing chord-extensions. Figure 20(a) presents the maximum lift coefficient for various inboard-end locations of a  $0.15c$  extension with the effect of added wing area being shown. A chord-extension having its inboard end at the most desirable position (as established by considerations of longitudinal stability) produces an increase of about 23 percent in maximum lift coefficient, with about 5 percent being attributed to the added wing area provided by the extensions.

A small increase in the minimum drag resulted from the addition of chord-extensions. For a given lift coefficient, the chord-extensions decreased the drag at the higher lift coefficients, probably because of alleviation of the tip-separation effects (see refs. 1 to 4).

Effect of wing chord-extension span.- Several tests were made to determine the effect of chord-extension span for chord-extensions having their inboard ends located at the  $0.65b/2$  position, which seemed about optimum from the results shown in figure 8. Except for the results on the chord-extension with the smallest span ( $0.05b/2$ ), these data (fig. 9) show essentially the same improvement to the stability as obtained with the chord-extension extending to the wing tip. When the chord-extension span is reduced to 5 percent wing semispan the unstable break in the pitching-moment curve again is experienced and the resulting curve is very similar to that obtained with a fence at  $0.60b/2$ . (See fig. 10.) There is however a small amount of instability noted for the 25-percent-span chord-extension (fig. 9) at lift coefficients between 0.3 and 0.5. It is believed that the interference effects between the tip vortex and a vortex generated at the outboard end of the chord-extension causes this small change in stability. Other data on this model (circular-arc wing) indicate that the various fences tried have not been powerful enough to eliminate completely the instability at high lifts. (See ref. 7.)

The increase in maximum lift coefficient observed for chord-extensions with spans extending to the tip was maintained as the span was reduced to 5 percent of the wing semispan, at which point the

characteristics reverted toward those of the clean-wing configuration (fig. 9) and also were similar to those obtained with a wing fence located at the  $0.60b/2$  position (fig. 10). Evidently the small-span chord-extension or the wing fence is not powerful enough to maintain a high tip loading on the present wing and results in the lower lift noted.

Variation in chord-extension span for an extension having the inboard end located at the optimum spanwise position did not alter the drag characteristics appreciably, except when the span was reduced to  $0.05b/2$ ; where the high-lift drag was similar to that of the clean wing and to that obtained with a fence located at the  $0.60b/2$  position. (See figs. 9 and 10.)

Effect of chord-extension overhang.- In order to determine the effect of overhang (percent wing chord) of the chord-extensions, several tests were made with the overhang reduced from 15 percent to 10 percent of the local wing chord (measured perpendicular to the 50-percent-chord line) for chord-extensions having their inboard-end locations at the  $0.65b/2$  position. These tests were made for both a 20- and 35-percent-span chord-extension. These data (fig. 11) show the 0.15c chord-extension to be slightly better, the greater improvement in stability being obtained for the chord-extension having a 35-percent span.

Effect of chord-extensions in combination with leading-edge flap deflection.- Unpublished data have shown that substantial gains in  $L/D$  can be obtained by wing chord-extensions in combination with wing leading-edge flap deflection. Results of reference 7 have shown that  $C_{L_{max}}$ , with plain trailing-edge flaps deflected, could be increased considerably by deflecting the wing leading edge over a large portion of the wing span. Inasmuch as leading-edge deflection alone did not provide satisfactory stability characteristics, the investigation of a combination of wing chord-extension and leading-edge flap deflection was adopted to determine if satisfactory stability characteristics and substantial gains in  $C_{L_{max}}$  could be achieved simultaneously. The flap-neutral and flaps-deflected tests were made at Reynolds numbers of  $2.2 \times 10^6$  and  $1.62 \times 10^6$ , respectively.

When the outer 60 percent of the wing leading edge with a 35-percent-semispan chord-extension on the tip portion was deflected, the longitudinal stability in the high-lift range decreased with increased nose-flap deflection, becoming unstable at the higher nose-flap deflections for both the plain trailing-edge flaps-neutral and flaps-deflected configurations (see figs. 12(a), 12(b), and 20(c)). With the plain trailing-edge flap deflected, data were not obtained with the nose flaps neutral (fig. 12(b)); however, if the assumption is made that the

stability and  $C_{L_{max}}$  characteristics are essentially the same for both a 35-percent and a 20-percent-span chord-extension (as was found to be true for the flaps-neutral case), the data of figure 15(b) can be compared with that of figure 12(b). This comparison indicates that, for small nose-flap deflections of about  $8^\circ$ , the  $C_{L_{max}}$  is increased from 0.95 to 1.06 while still maintaining satisfactory stability characteristics. Further gains in  $C_{L_{max}}$  are obtained by larger nose-flap deflections, but the model becomes unstable above deflections of about  $12^\circ$ .

For a nose-flap deflection of  $18^\circ$ , increasing the span of the leading-edge flap toward the plane of symmetry (fig. 13) improved the stability in the high-lift-coefficient range and extended the pitching-moment break to a higher lift coefficient for configurations with plain trailing-edge flaps deflected. However, when the chord-extension portion of the leading edge was undeflected, with the inboard portions being deflected  $18^\circ$  and with plain trailing-edge flaps deflected  $50^\circ$  (fig. 13), the pitching-moment curve had an unstable break at stall similar to that noted for the wing without a chord-extension (fig. 15(a)), although the break occurred at a higher lift coefficient.

It can be seen from figure 12(b), for the plain trailing-edge flaps deflected  $50^\circ$ , that deflecting only the chord-extension portion of the leading edge produces small decreases in  $C_{L_{max}}$ . With the chord-extension portion of the nose flap deflected  $18^\circ$ , increasing the span of the nose flap toward the plane of symmetry (fig. 13) increased  $C_{L_{max}}$  by about 0.23 for full-span deflection. Deflecting only the plain trailing-edge flap  $50^\circ$  increased  $C_{L_{max}}$  about 0.09 over that which was realized from the clean-wing configuration (figs. 14 and 15).

For plain trailing-edge flaps either neutral or deflected (figs. 12(a) and 12(b)), deflecting the outer 60-percent-semispan portion of the nose flap decreased the drag due to lift; whereas deflecting only the chord-extension portion with trailing-edge flaps deflected increased the drag due to lift (fig. 12(b)). Figure 13 shows that, with the wing-tip portion of the nose flap deflected  $18^\circ$ , increasing the span of the nose flap toward the plane of symmetry decreased the drag due to lift for plain trailing-edge flaps deflected.

Effect of horizontal tail.- Changing the tail incidence does not appreciably affect the stability characteristics for either the flaps-neutral or flaps-deflected configurations. (See figs. 14 to 16.) The instability noted for the clean-wing configurations is eliminated by the addition of chord-extensions for all flap configurations tested, which, as previously mentioned, is mainly caused by improved flow over the wing tip. The data of figures 17 to 19, however, show that the addition of

chord-extensions (with or without leading-edge flap deflection) provides a small improvement in stability by changing the downwash and dynamic-pressure characteristics at the tail. The horizontal-tail increment of pitching moment caused by chord-extensions with the plain flaps neutral is practically negligible below an angle of attack of  $12^\circ$  (fig. 19) and is small at higher angles. When the plain flaps are deflected  $50^\circ$ , however, the downwash at the tail produces a favorable pitching-moment increment at angles of attack above  $5^\circ$ .

#### Effect of Chord-Extension Span and Overhang on the Lateral-Stability Parameters

Addition of one of the better chord-extensions (from longitudinal stability considerations) to the complete model with flaps undeflected did not appreciably affect  $C_{Y\beta}$  and  $C_{N\beta}$ . (See fig. 21.) The chord-extensions did, however, increase the effective-dihedral parameter  $C_{l\beta}$  in the moderate- to high-lift-coefficient range, probably because of their ability to reduce stalling in the tip region. The smaller-span chord-extensions generally give somewhat larger values of  $C_{l\beta}$  in the high lift range.

#### CONCLUSIONS

The results of tests of wing leading-edge chord-extensions in conjunction with several flap configurations on a complete model having a  $40^\circ$  sweptback circular-arc wing of aspect ratio 4 and taper ratio 0.50 indicate the following conclusions:

1. The degree of effectiveness of the chord-extension in improving longitudinal stability characteristics is mainly dependent upon the spanwise inboard-end location of such a device. For a suitable inboard-end location (0.65 semispan from plane of symmetry for the present model) the chord-extension span could be changed from 0.35 semispan to 0.15 semispan with little change in longitudinal stability or lift characteristics.
2. Reduction of the chord-extension overhang from 15 percent to 10 percent of the local chord caused only a very slight decrease in the effectiveness of the device in improving the longitudinal stability.
3. With plain trailing-edge flaps retracted, use of a leading-edge chord-extension appeared to provide a considerable advantage over a leading-edge fence located at the spanwise position (0.60 wing semispan) of the inboard end of the chord-extension. The fence provided essentially

no increase in maximum lift and allowed an unstable break in the pitching-moment curve at the stall; whereas the chord-extension increased the maximum lift coefficient by about 23 percent and eliminated any serious loss in longitudinal stability throughout the lift range.

4. With a combination of a leading-edge chord-extension and deflection of a leading-edge flap, substantial improvements in drag due to lift and in maximum lift coefficient could be obtained while maintaining favorable high-lift pitching-moment characteristics when the plain trailing-edge flaps were neutral or deflected. For such a configuration it was essential that the leading-edge flaps include the chord-extension and also extend an appreciable distance inboard of the chord-extension.

5. The use of chord-extensions for the configuration having plain trailing-edge and leading-edge flaps neutral increased the effective dihedral in the moderate- to high-lift-coefficient range but did not appreciably affect the lateral-force or yawing-moment parameters.

Langley Aeronautical Laboratory  
National Advisory Committee for Aeronautics  
Langley Field, Va.

## REFERENCES

1. Lowry, John G., and Schneiter, Leslie E.: Investigation at Low Speed of the Longitudinal Stability Characteristics of a  $60^\circ$  Swept-Back Tapered Low-Drag Wing. NACA TN 1284, 1947.
2. Furlong, G. Chester: Exploratory Investigation of Leading-Edge Chord-Extensions To Improve the Longitudinal Stability Characteristics of Two  $52^\circ$  Sweptback Wings. NACA RM L50A30, 1950.
3. Jaquet, Byron M.: Effects of Chord Discontinuities and Chordwise Fences on Low-Speed Static Longitudinal Stability of an Airplane Model Having a  $35^\circ$  Sweptback Wing. NACA RM L52C25, 1952.
4. Furlong, G. Chester, and McHugh, James G.: A Summary and Analysis of the Low-Speed Longitudinal Characteristics of Swept Wings at High Reynolds Numbers. NACA RM L52D16, 1952.
5. Gillis, Clarence L., Polhamus, Edward C., and Gray, Joseph L., Jr.: Charts for Determining Jet-Boundary Corrections for Complete Models in 7- by 10-Foot Closed Rectangular Wind Tunnels. NACA ARR L5G31, 1945.
6. Thom, A.: Blockage Corrections in a Closed High-Speed Tunnel. R. & M. No. 2033, British A.R.C., 1943.
7. Weil, Joseph, Comisarow, Paul, and Goodson, Kenneth W.: Longitudinal Stability and Control Characteristics of an Airplane Model Having a  $42.8^\circ$  Sweptback Circular-Arc Wing With Aspect Ratio 4.00, Taper Ratio 0.50, and Sweptback Tail Surfaces. NACA RM L7G28, 1947.

TABLE I.- PHYSICAL CHARACTERISTICS OF THE TEST MODEL

Characteristics	Wing	Horizontal tail	Vertical tail
Area, sq ft	12.70	2.06	2.26
Span, in.	85.50	34.00	20.08
Sweepback, $\Lambda_c/4$ , deg	40.0	39.9	31.5
Aspect ratio	4.00	3.87	1.23
Taper ratio	0.50	0.49	0.31
Dihedral, deg	3.5	0	
Angle of incidence, deg	3		
Mean aerodynamic chord, in.	22.15		
Root chord, in.	28.50	11.75	24.74
Theoretical tip chord, in.	14.25	5.75	7.74
Root airfoil section	10-percent-thick circular arc	NACA 65-008	NACA 27-010
Tip airfoil section	10-percent-thick circular arc	NACA 65-008	NACA 27-008


 NACA

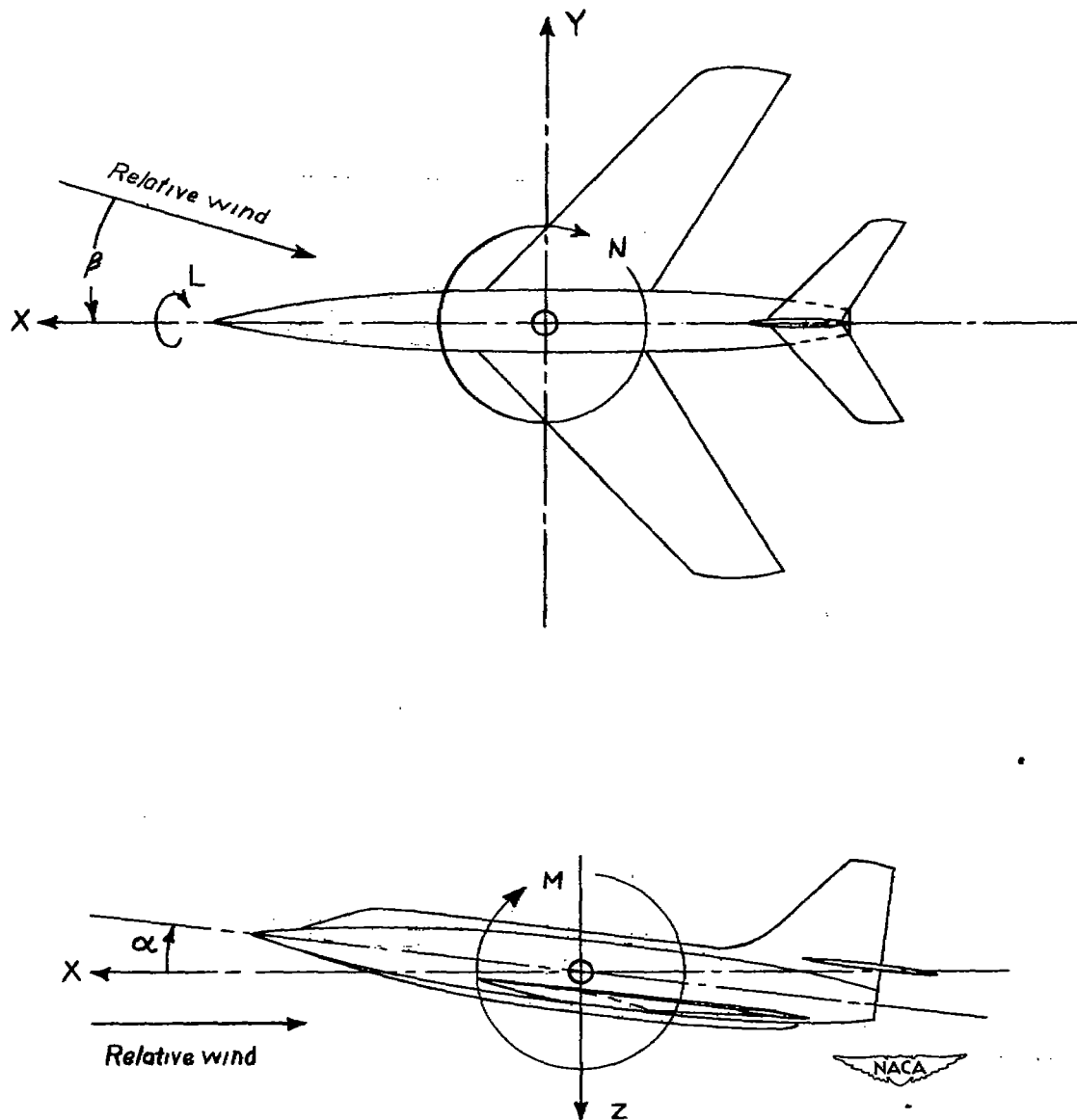


Figure 1.- System of axes. Positive values of forces, moments, and angles are indicated by arrows.

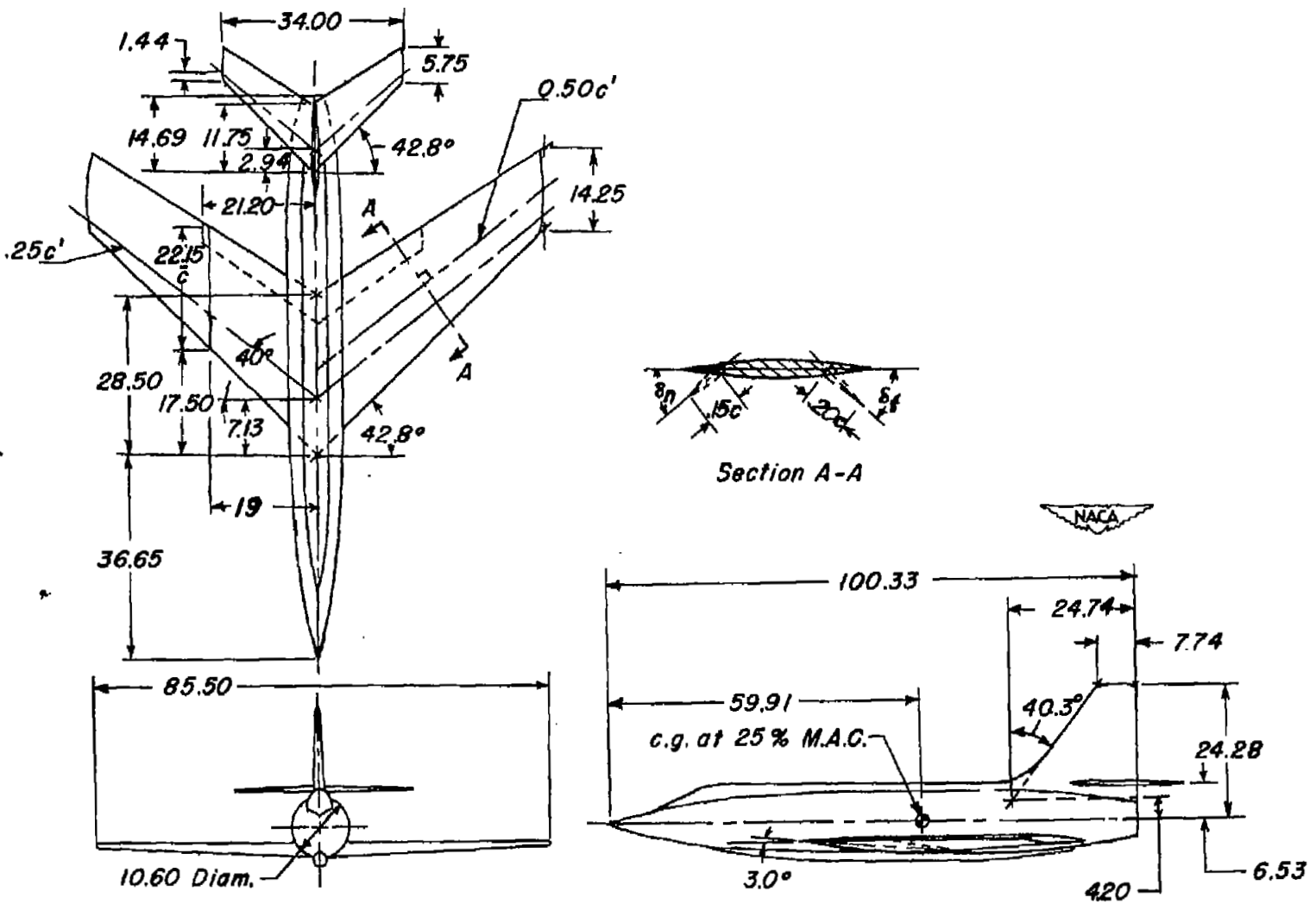


Figure 2.- General arrangement of the test model. All dimensions are in inches.

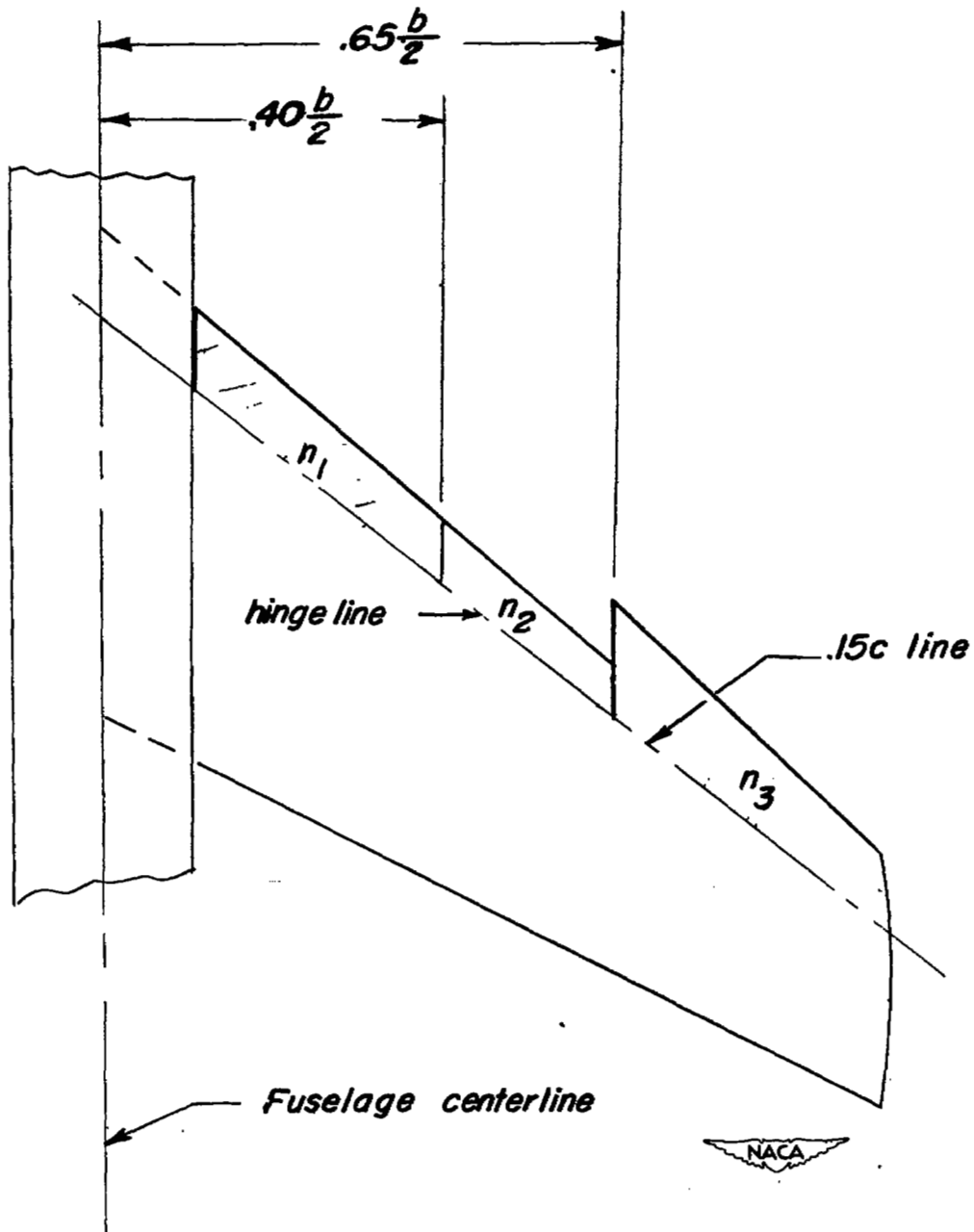


Figure 3.- Sketch showing deflectable portions of wing leading edge.

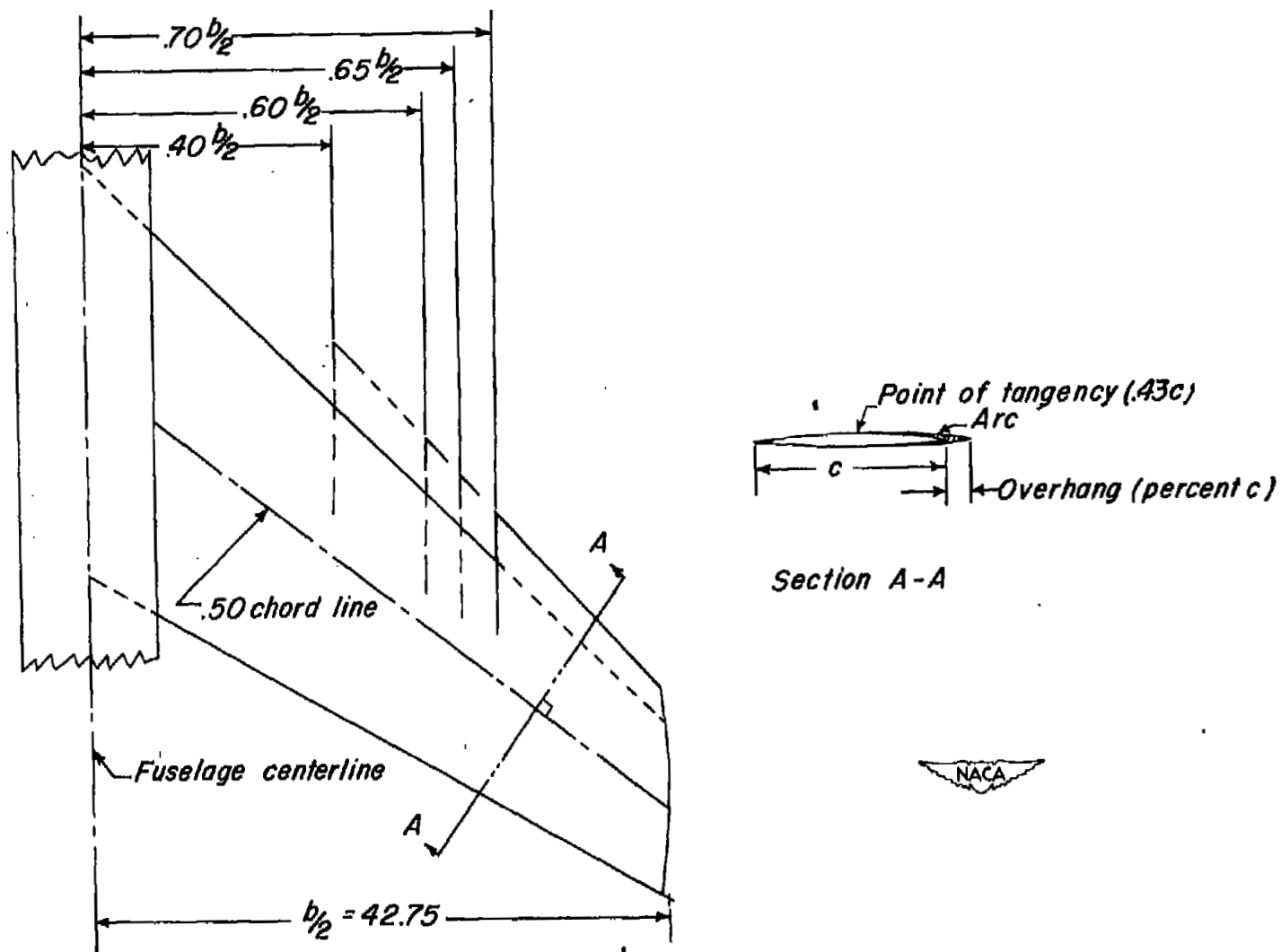


Figure 4.- Details of chord-extensions measured from the wing tip to various spanwise stations.

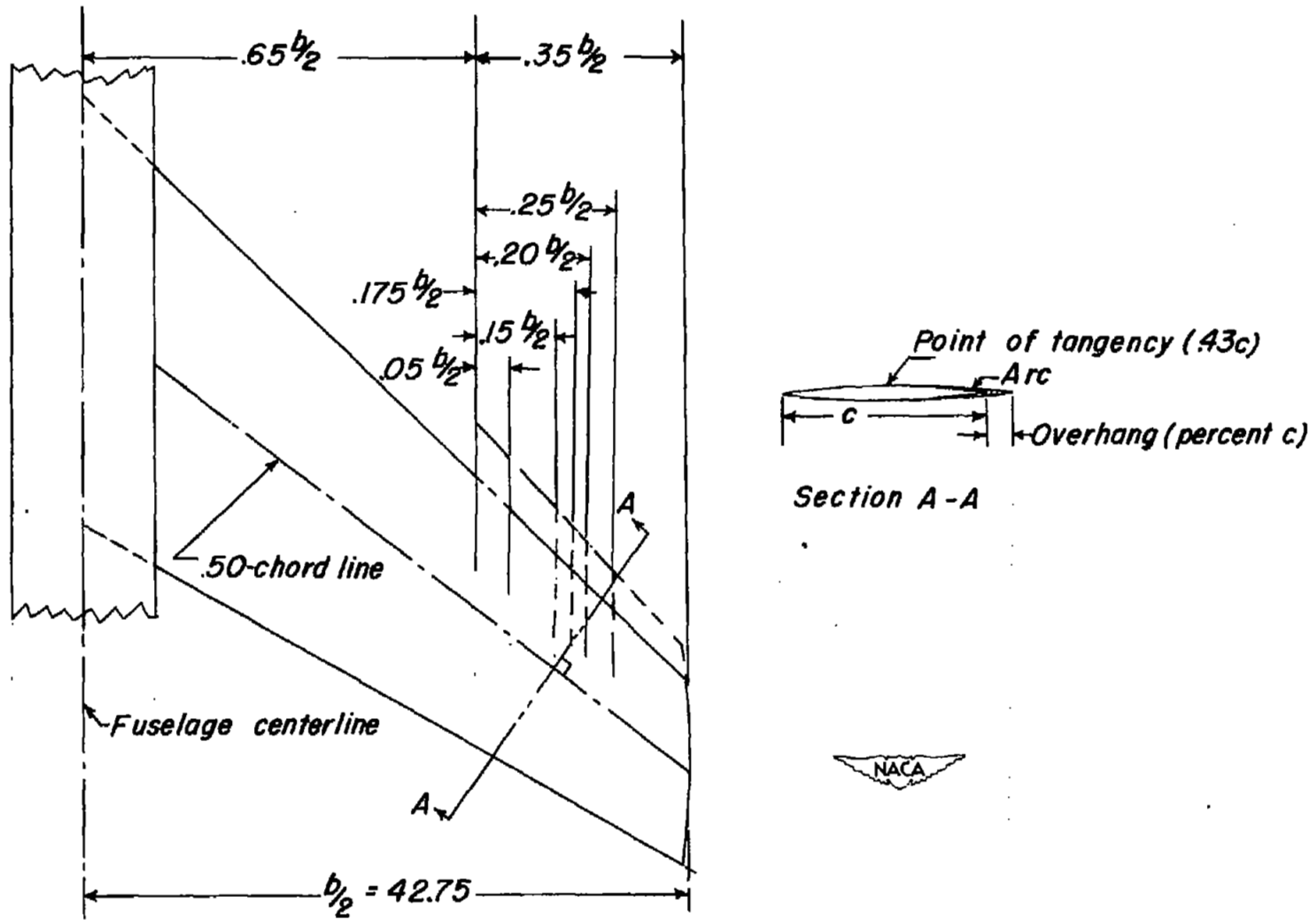


Figure 5.- Details of chord-extensions measured from an inboard-end location of  $0.65b/2$ .

*Fence located streamwise at  $0.60b/2$*

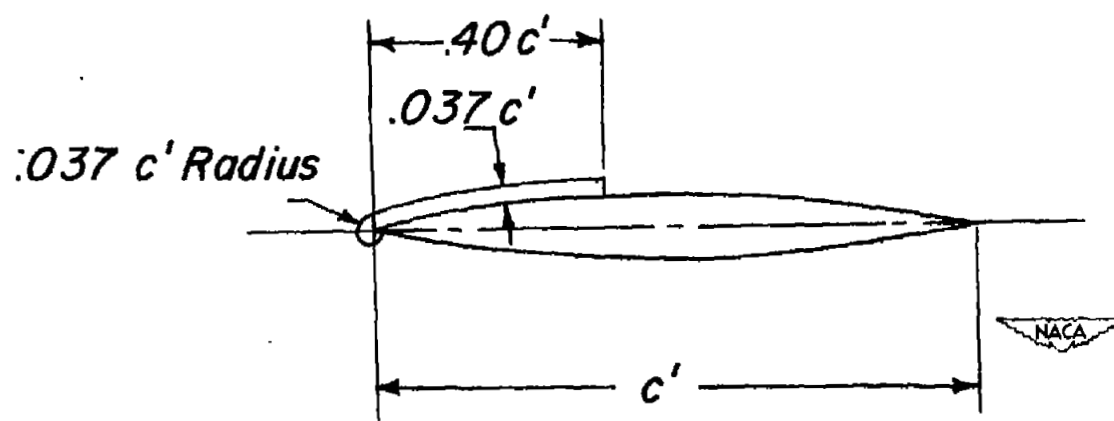
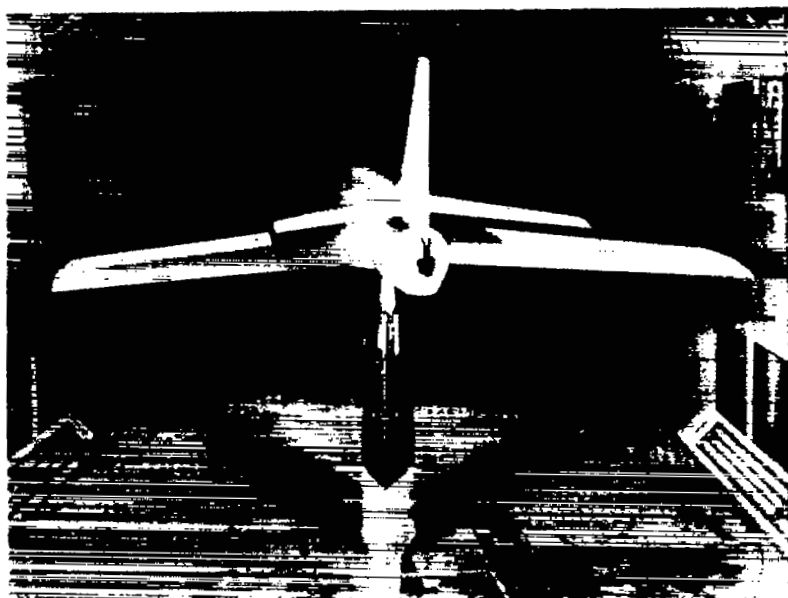
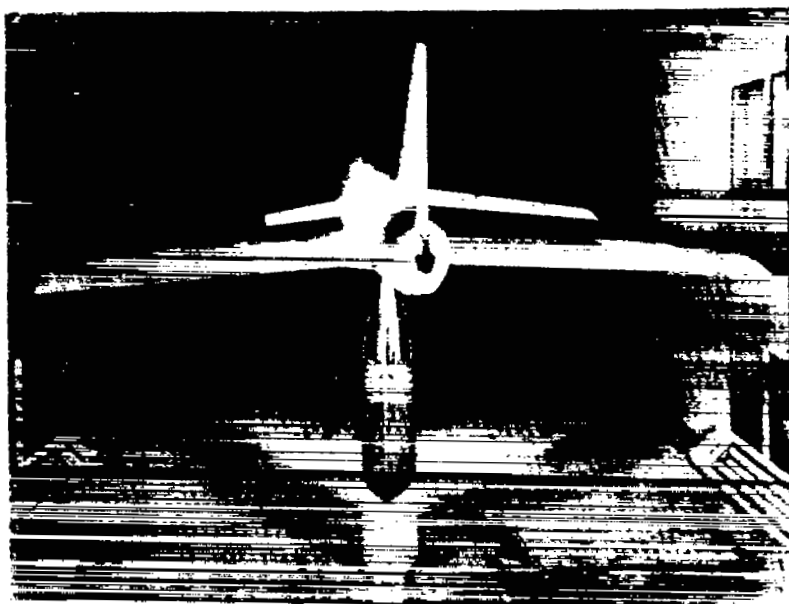


Figure 6.- Details of the wing fence located on the circular-arc wing.



(a) Chord-extension inboard-end location,  $0.40b/2$ ; outboard-end extended to wing tip; chord extended,  $0.15c$ .

NACA  
L-69673



(b) Chord-extension inboard-end location,  $0.65b/2$ ; chord-extension span,  $0.20b/2$ ; chord extended,  $0.15c$ .

NACA

Figure 7.- Photograph of test model as mounted in tunnel. L-69760

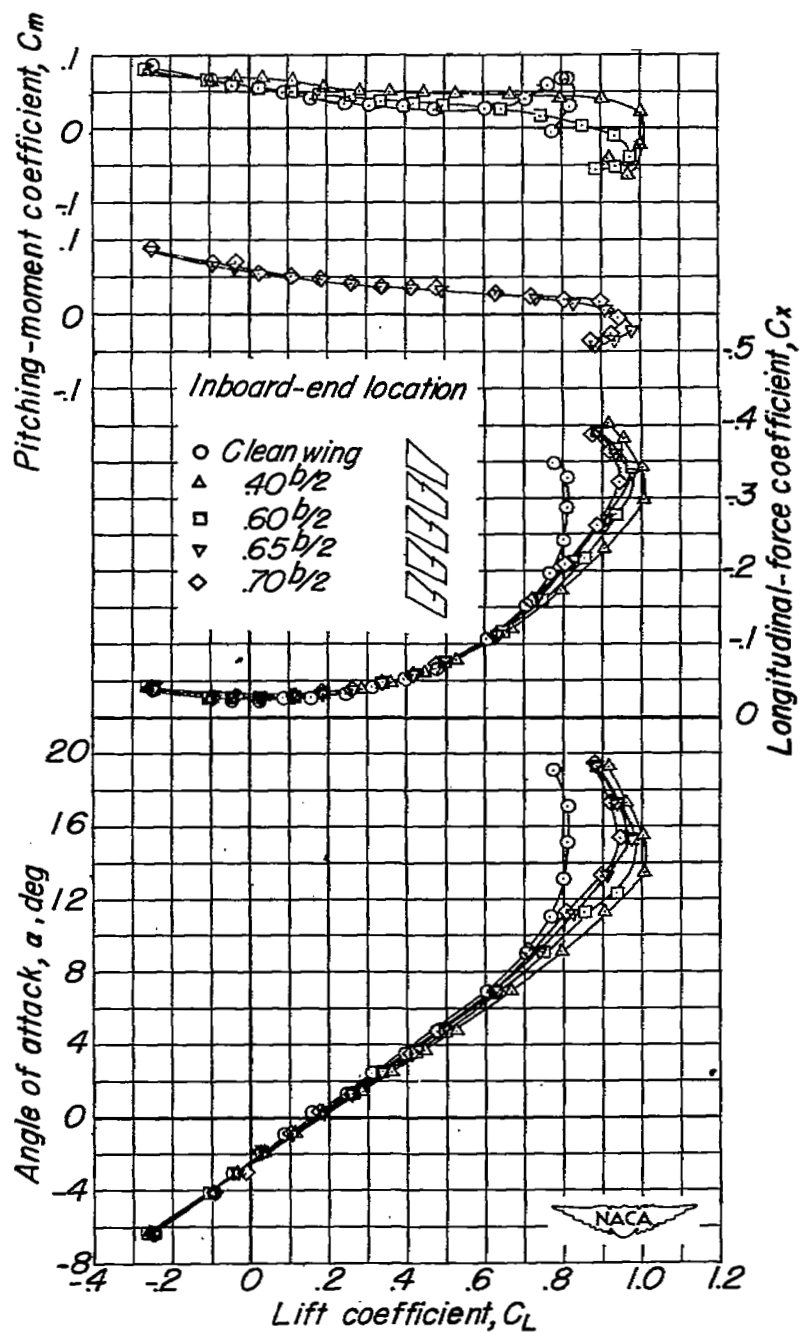


Figure 8.- The effect of inboard-end location of chord-extensions on the aerodynamic characteristics of the test model. Chord-extension span extends to wing tip; overhang  $0.15c$ ;  $i_t = 0^\circ$ ;  $\delta_f = 0^\circ$ ;  $\delta_{n_1} = 0^\circ$ ;  $\delta_{n_2} = 0^\circ$ ;  $\delta_{n_3} = 0^\circ$ .

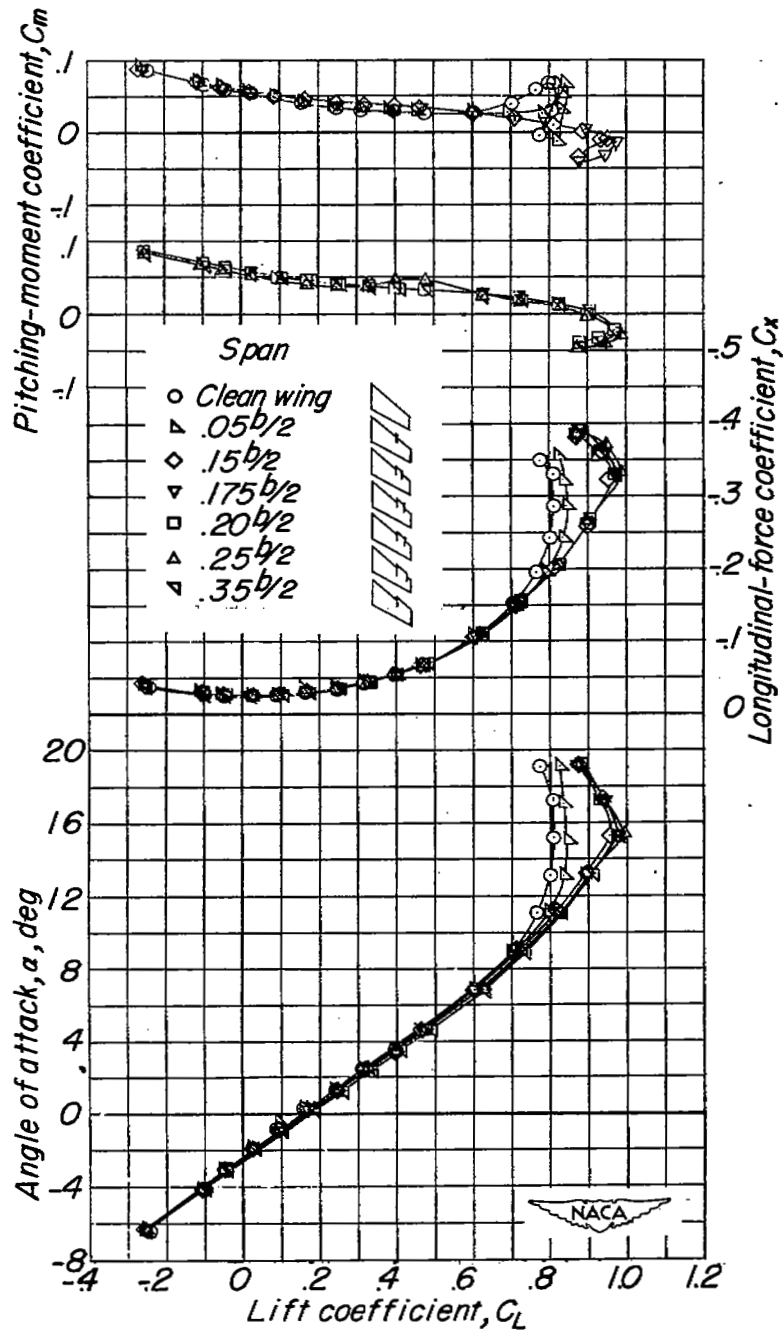


Figure 9.- The effect of chord-extension span on the aerodynamic characteristics of the test model. Inboard-end location 65 percent wing semispan; overhang  $0.15c$ ;  $i_t = 0^\circ$ ;  $\delta_f = 0^\circ$ ;  $\delta_{n_1} = 0^\circ$ ;  $\delta_{n_2} = 0^\circ$ ;  $\delta_{n_3} = 0^\circ$ .

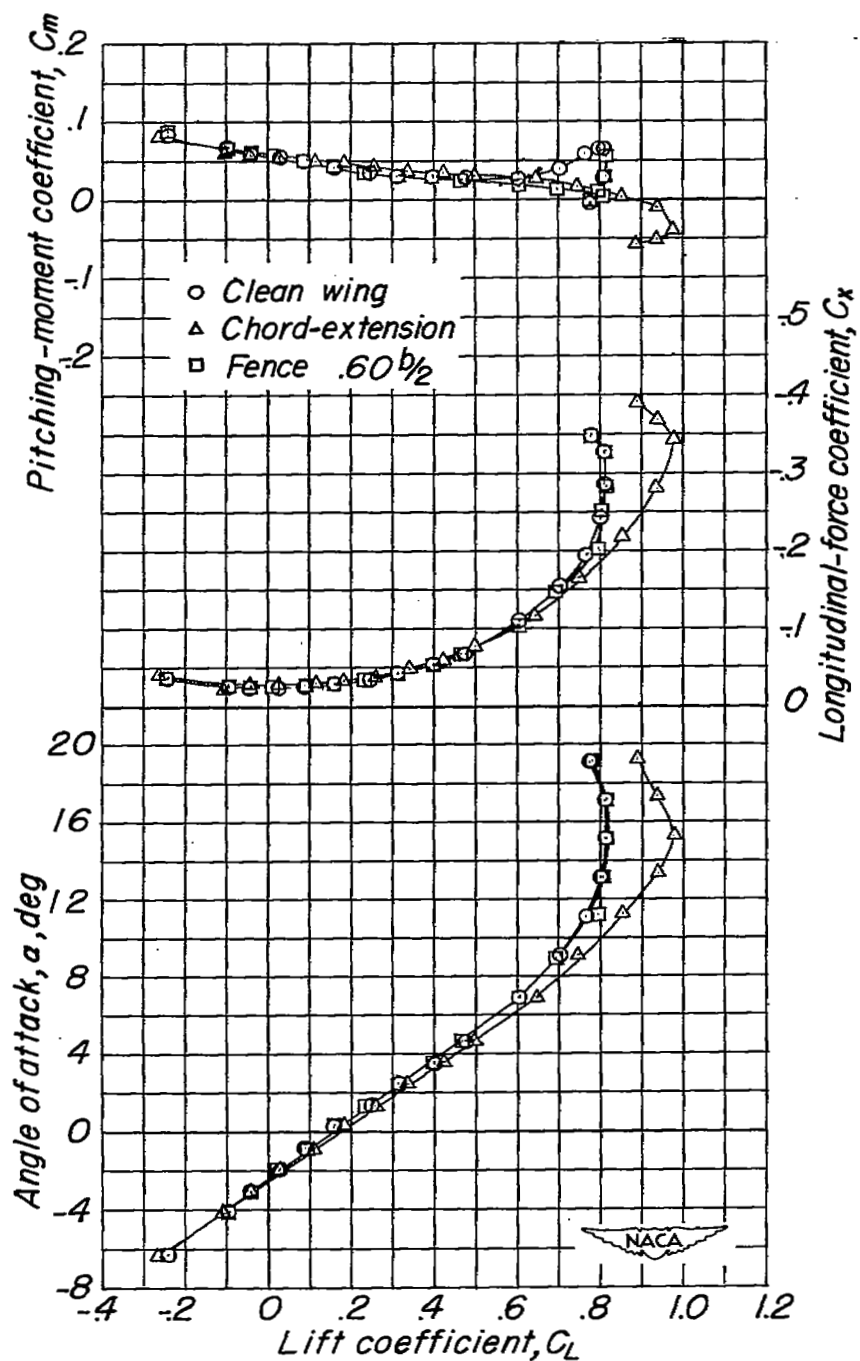
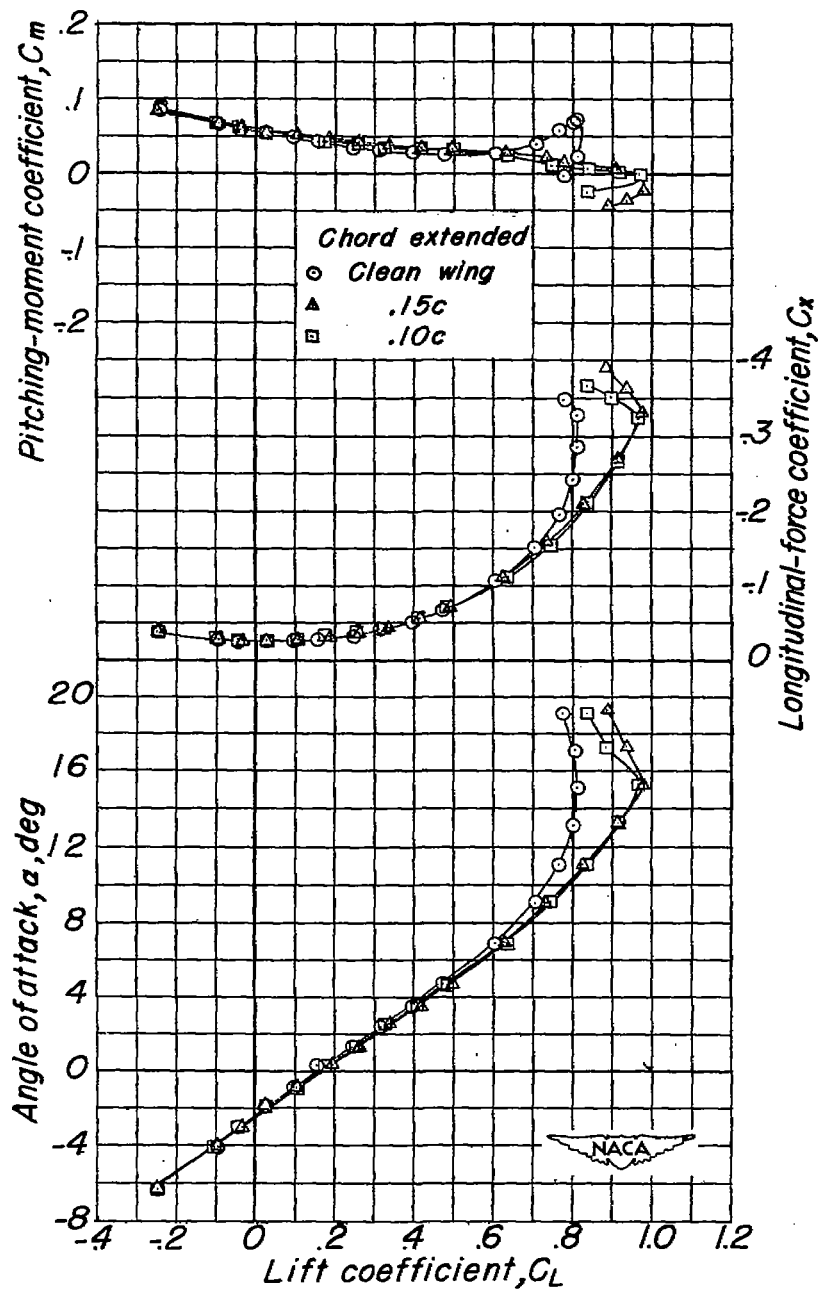
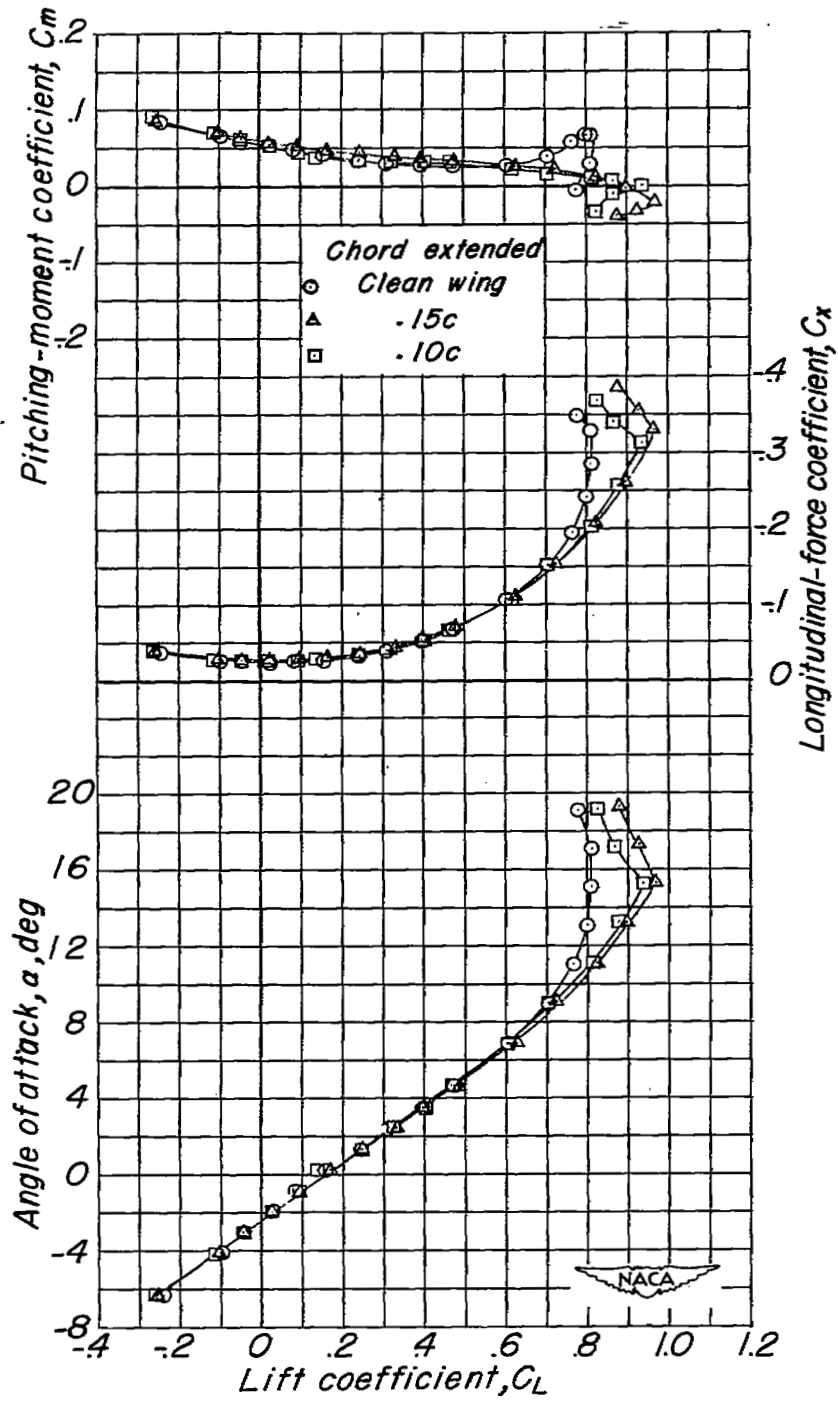


Figure 10.- Comparison of the effects of a wing fence and chord-extension on the aerodynamic characteristics of the test model. Chord-extension span extends from  $0.60b/2$  to wing tip; overhang,  $0.15c$ ;  $i_t = 0^\circ$ ;  $\delta_F = 0^\circ$ ;  $\delta_{n_1} = 0^\circ$ ;  $\delta_{n_2} = 0^\circ$ ;  $\delta_{n_3} = 0^\circ$ .



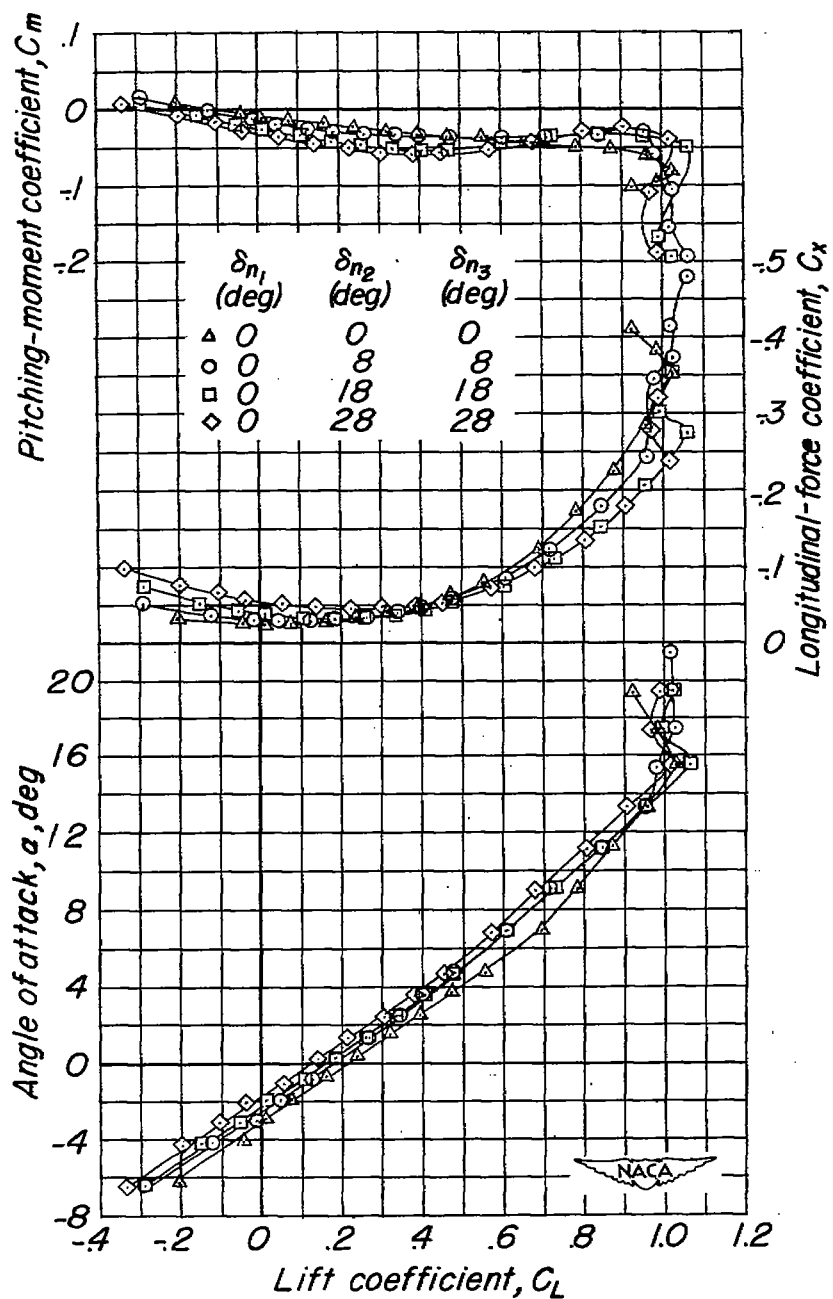
(a) Chord-extension span 35 percent wing semispan.

Figure 11.- The effect of chord-extension overhang (percent wing chord) on the aerodynamic characteristics of the test model. Inboard-end location 65 percent wing semispan;  $i_t = 0^\circ$ ;  $\delta_f = 0^\circ$ ;  $\delta_{n1} = 0^\circ$ ;  $\delta_{n2} = 0^\circ$ ;  $\delta_{n3} = 0^\circ$ .



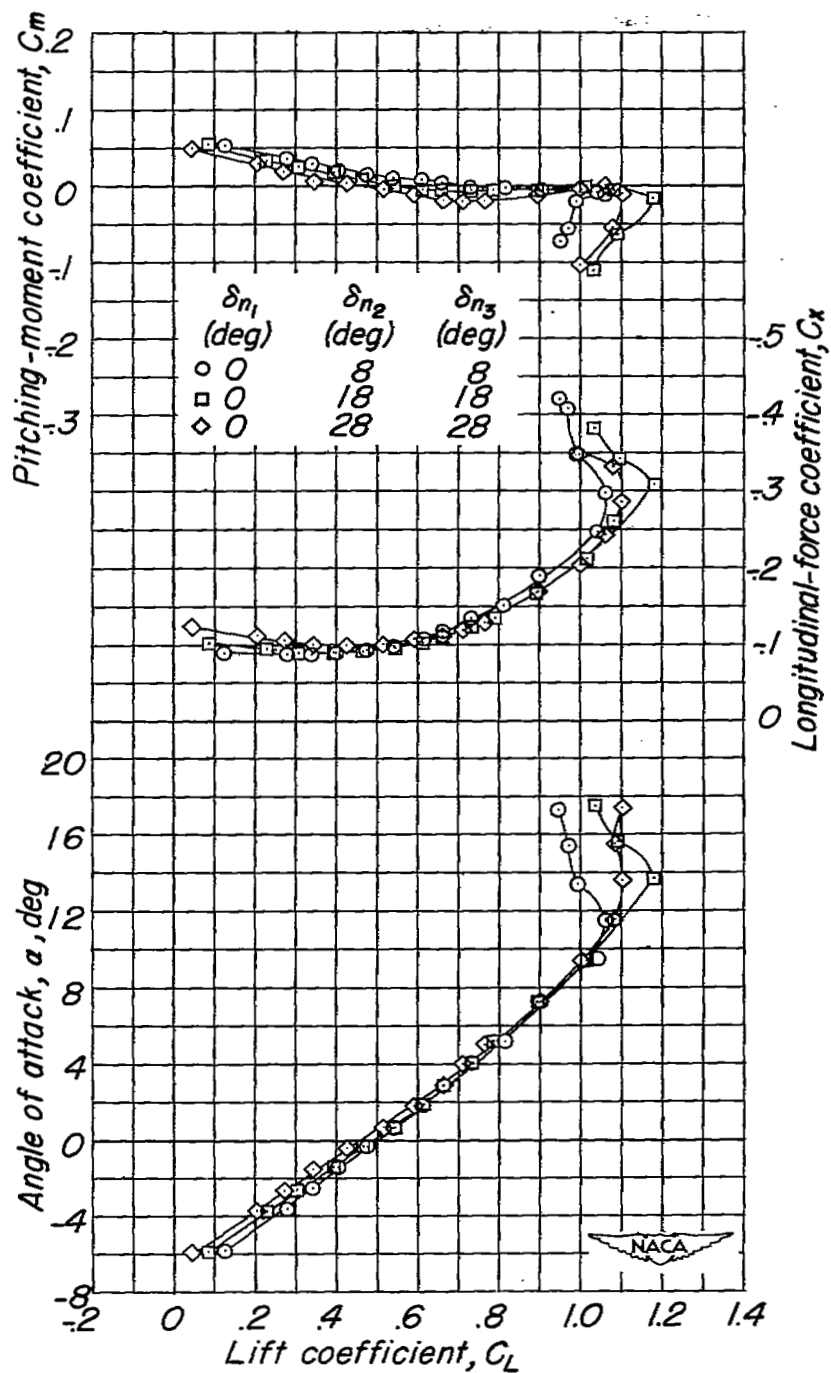
(b) Chord-extension span 20 percent wing semispan.

Figure 11.- Concluded.



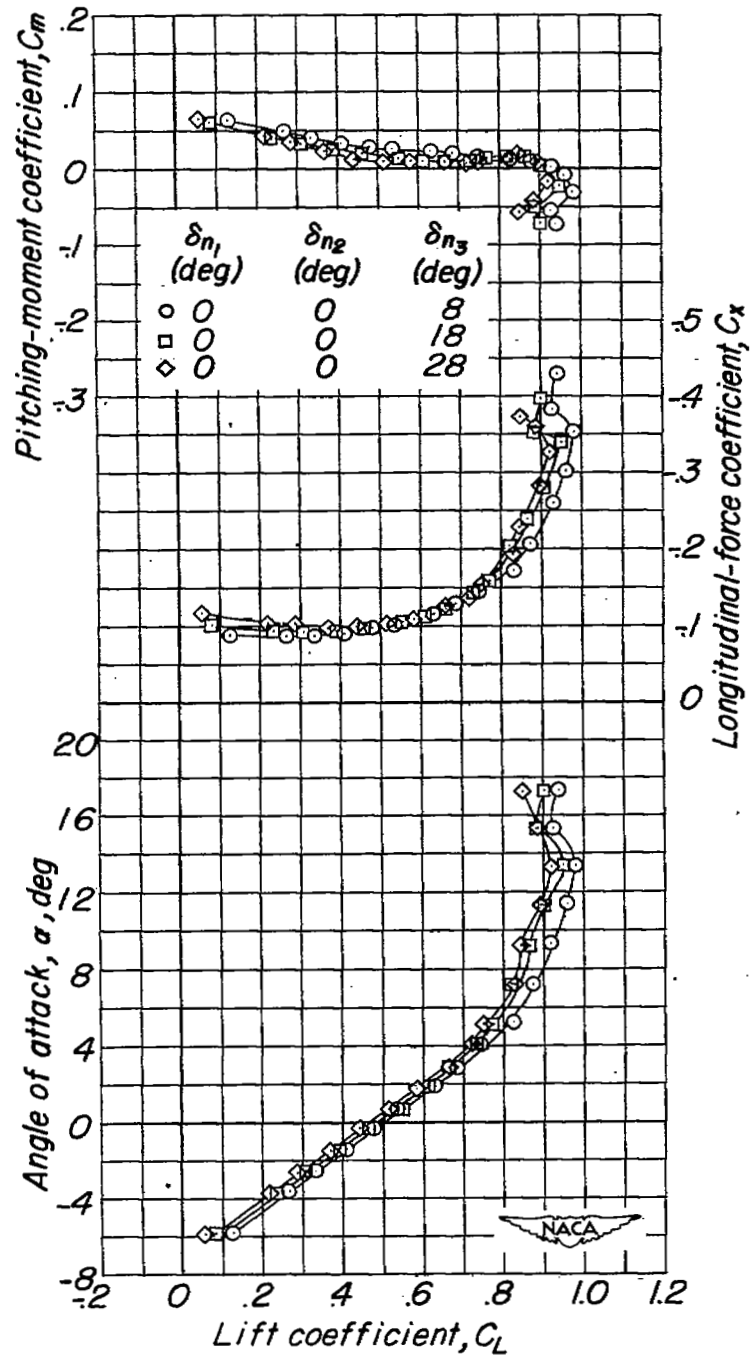
(a)  $\delta_f = 0^\circ$ ;  $i_t = 5^\circ$ .

Figure 12.- The effect of leading-edge deflection in conjunction with a chord-extension. Chord-extension span extends from  $0.65b/2$  to wing tip; overhang,  $0.15c$ .



(b)  $\delta_f = 50^\circ$ ;  $i_t = 0^\circ$ .

Figure 12.- Continued.



(b) Concluded.

Figure 12.- Concluded.

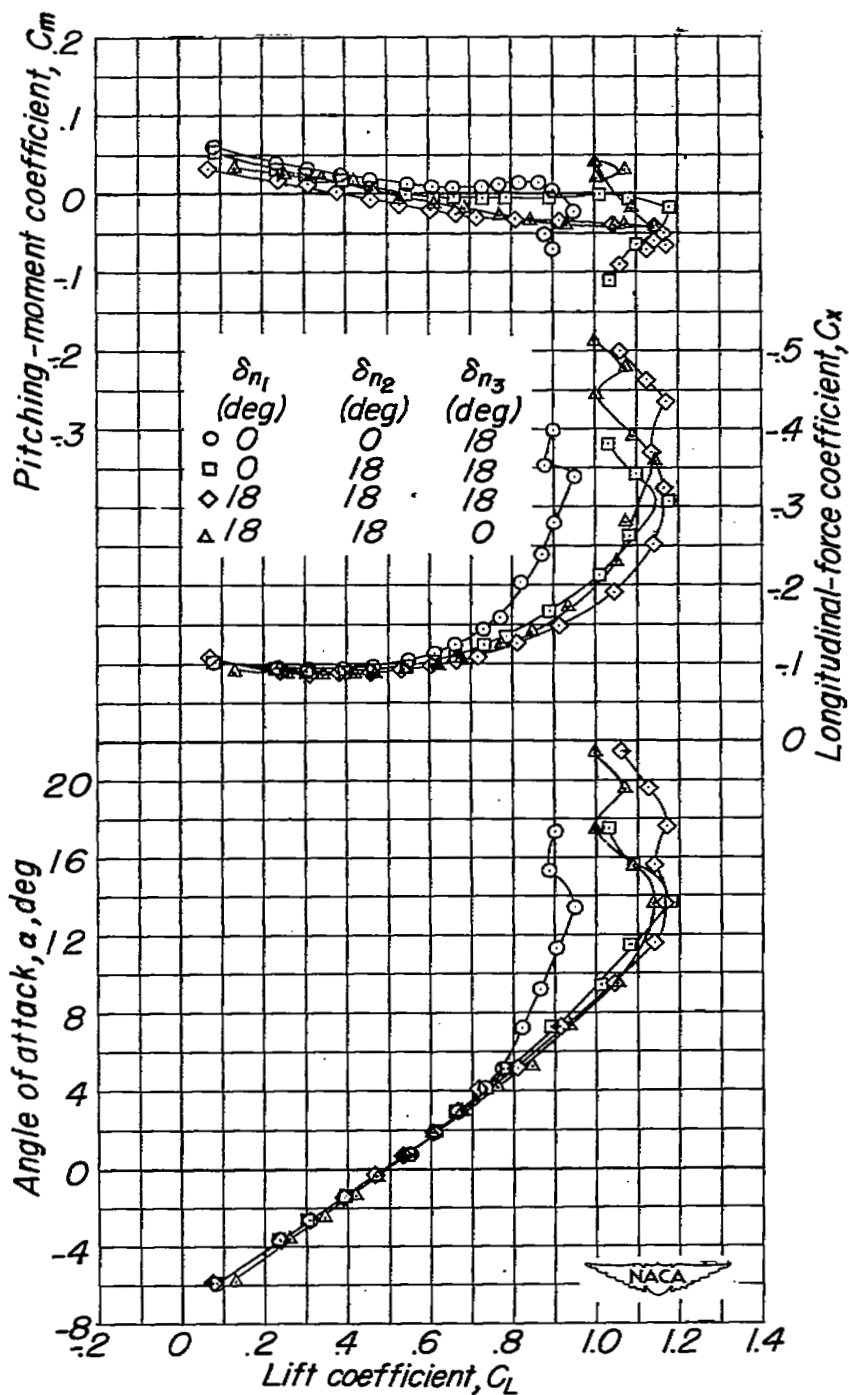
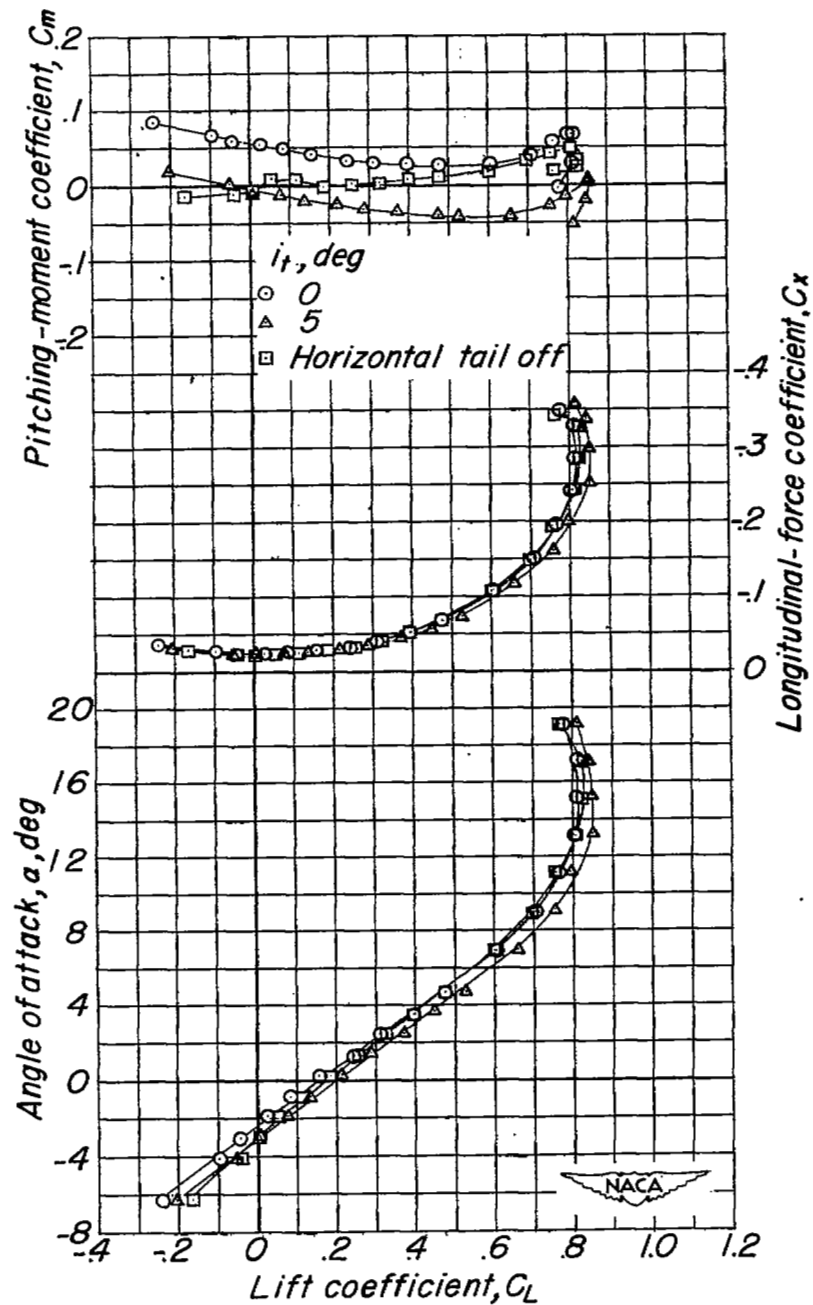
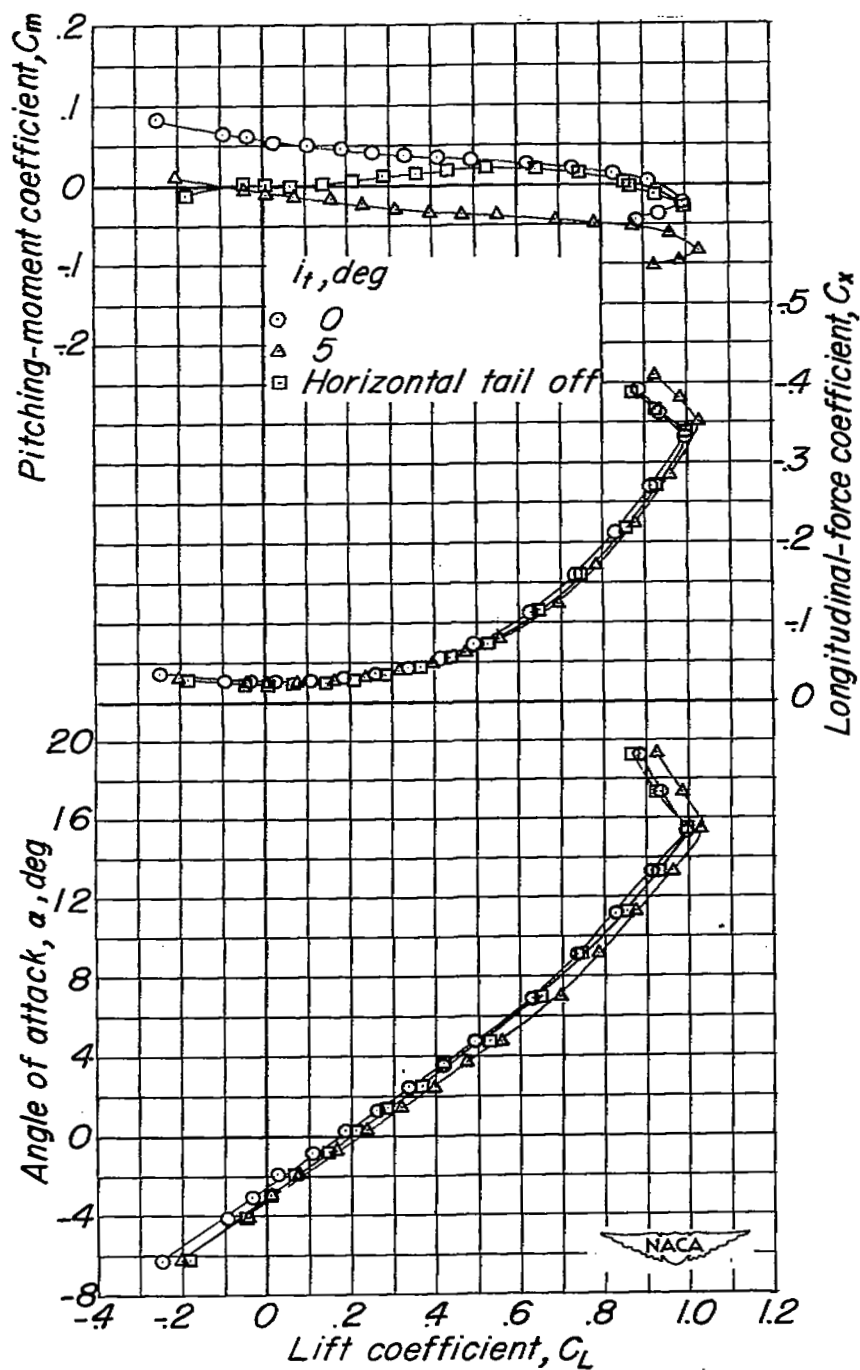


Figure 13.- The effect of leading-edge deflection in conjunction with a chord-extension. Chord-extension span extends from  $0.65b/2$  to wing tip; overhang,  $0.15c$ ;  $i_t = 0^\circ$ ;  $\delta_f = 50^\circ$ .



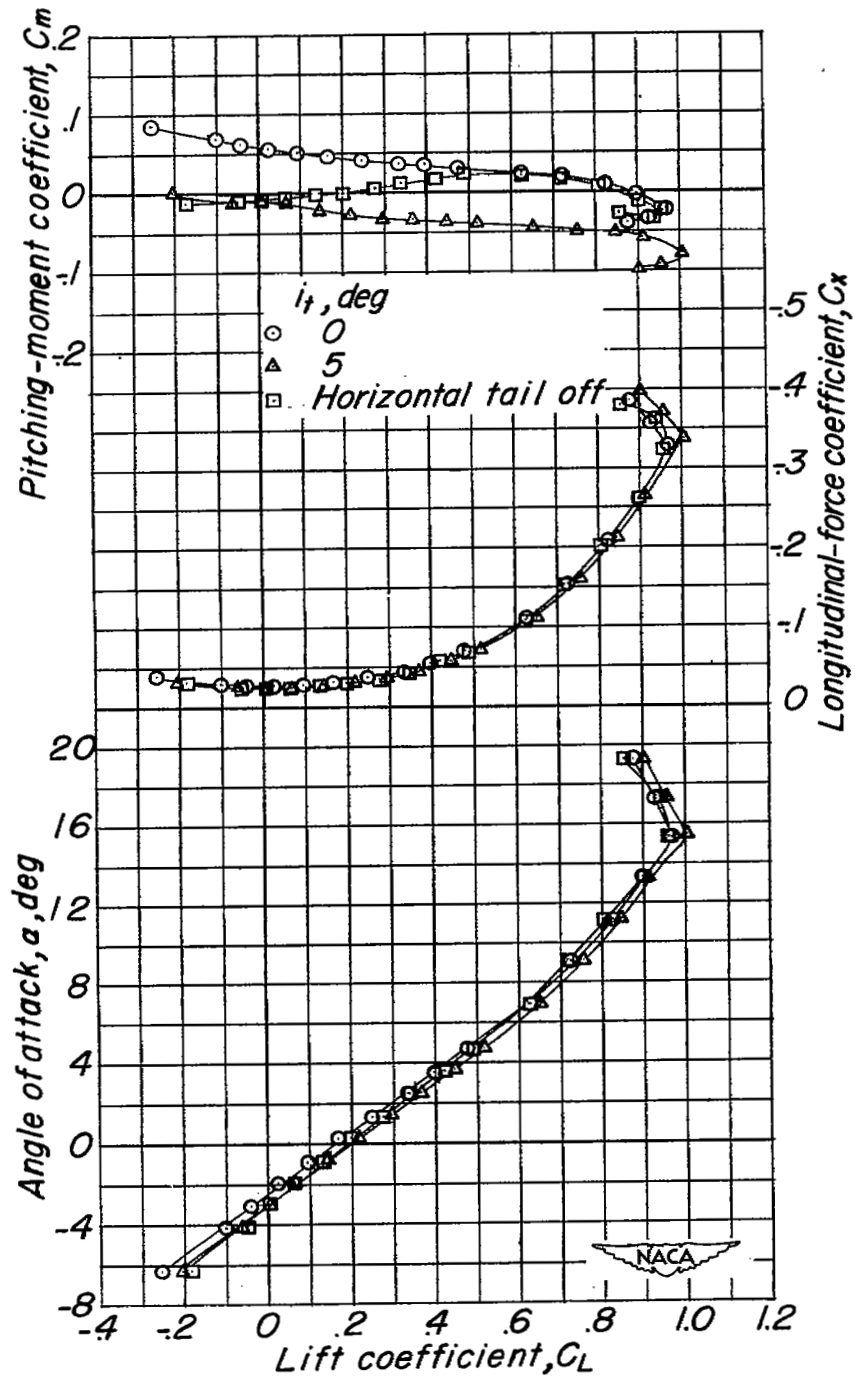
(a) Clean-wing model.

Figure 14.- The effect of tail on the aerodynamic characteristics of the clean-wing model and the model incorporating various chord-extension configurations.  $\delta_f = 0^\circ$ ;  $\delta_{n_1} = 0^\circ$ ;  $\delta_{n_2} = 0^\circ$ ;  $\delta_{n_3} = 0^\circ$ .



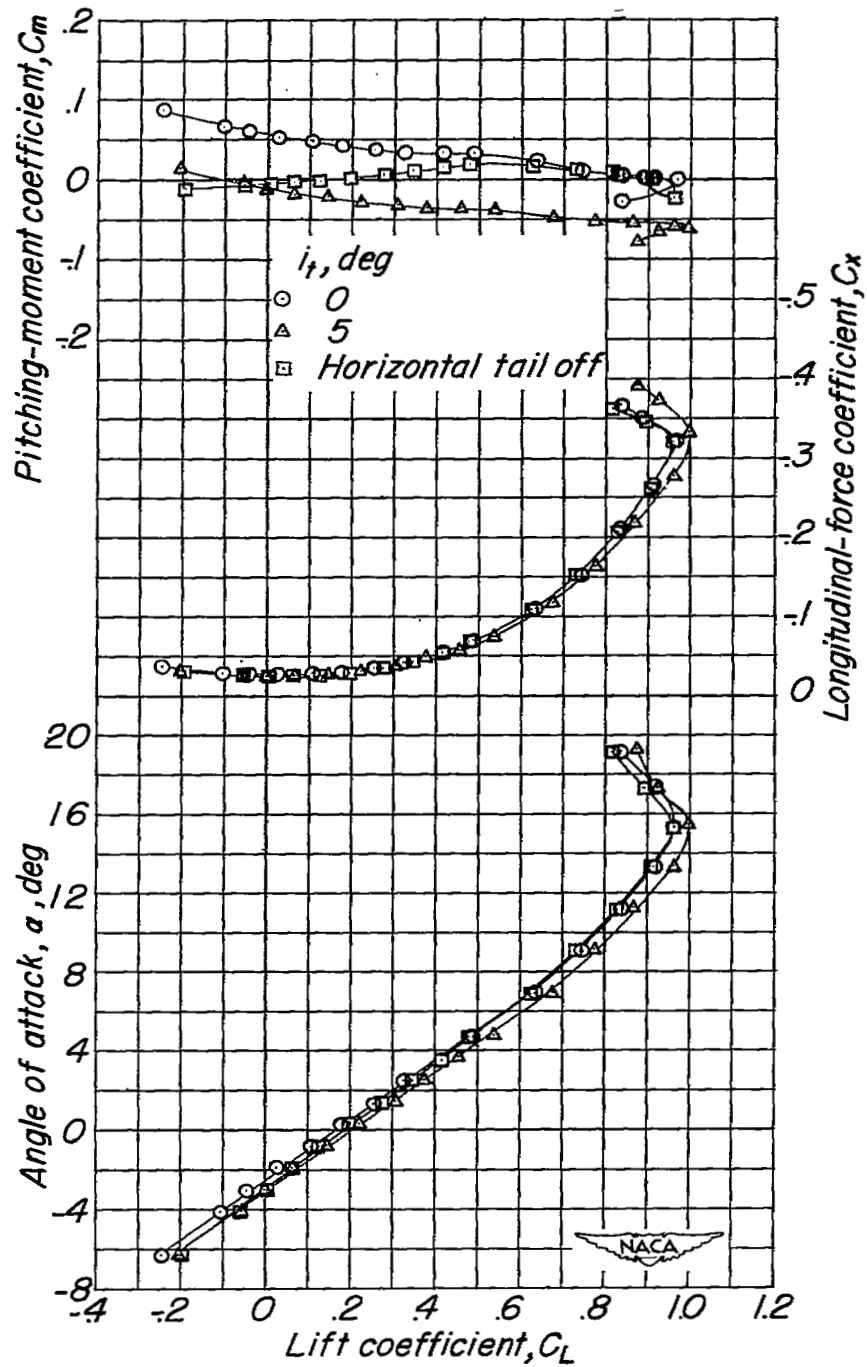
(b) Inboard-end chord-extension location, 65 percent wing semispan; chord-extension span, 35 percent wing semispan; overhang, 0.15c.

Figure 14.- Continued.



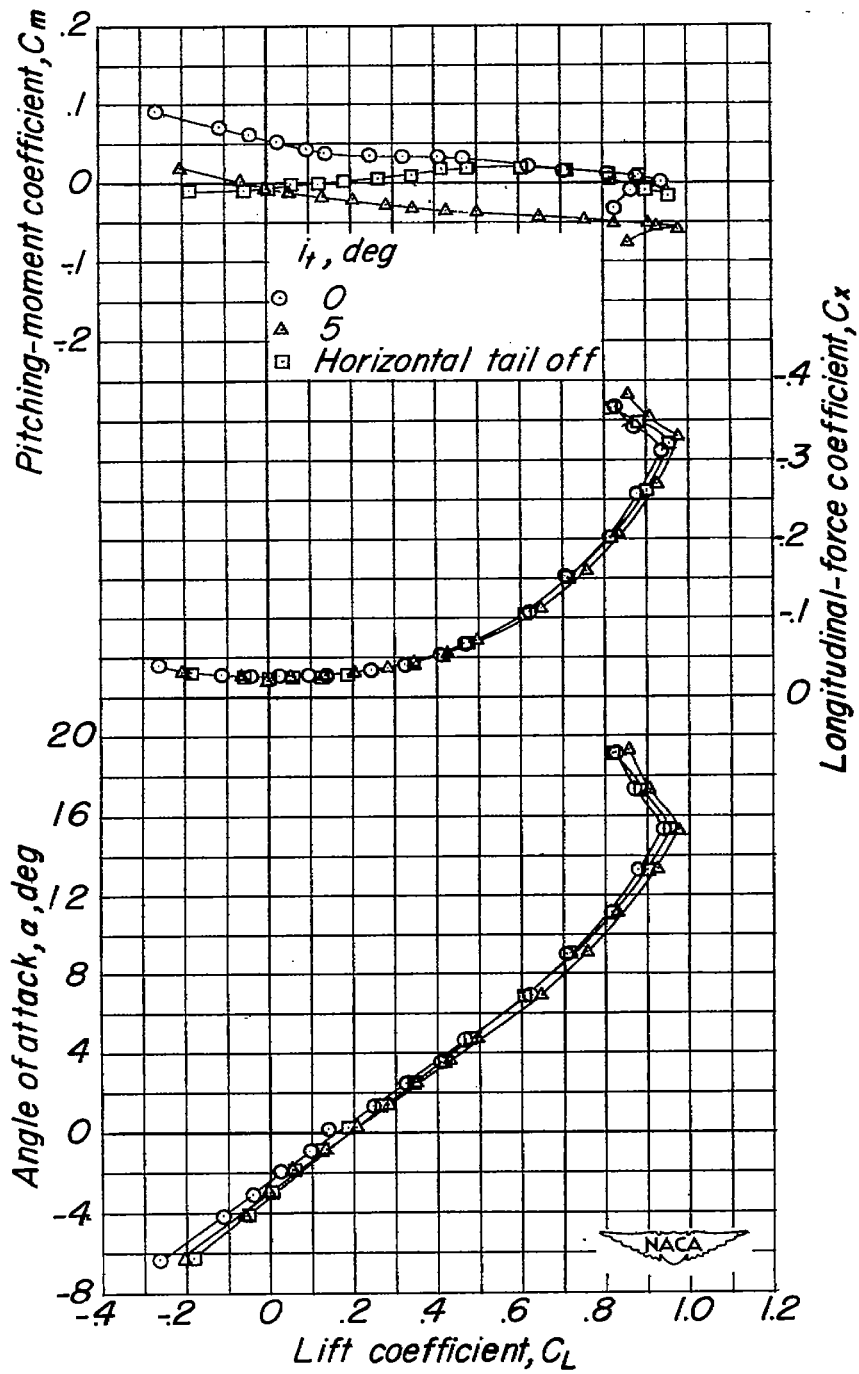
(c) Inboard-end chord-extension location, 65 percent wing semispan; chord-extension span, 20 percent wing semispan; overhang,  $0.15c$ .

Figure 14.- Continued.



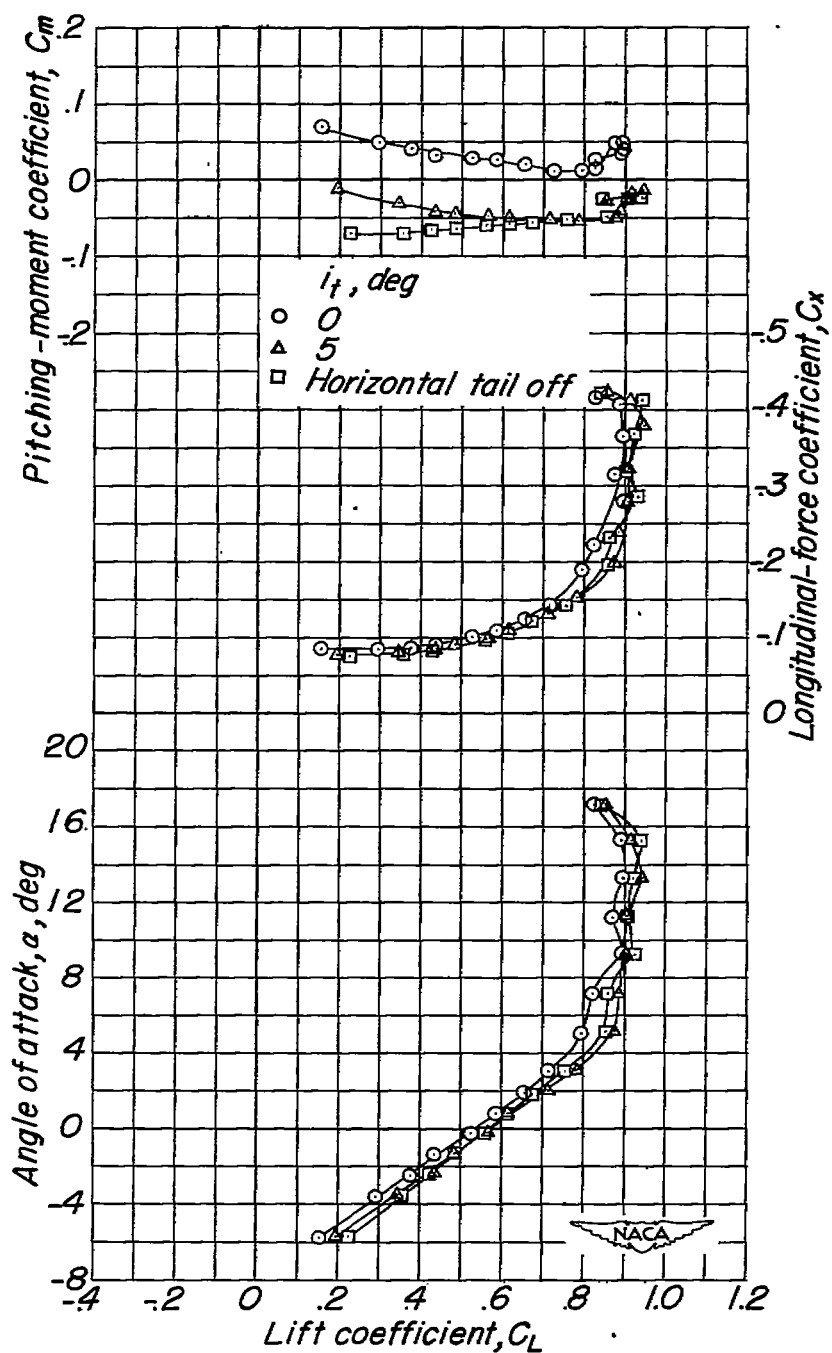
(d) Inboard-end chord-extension location, 65 percent wing semispan; chord-extension span, 35 percent wing semispan; overhang,  $0.10c$ .

Figure 14.- Continued.



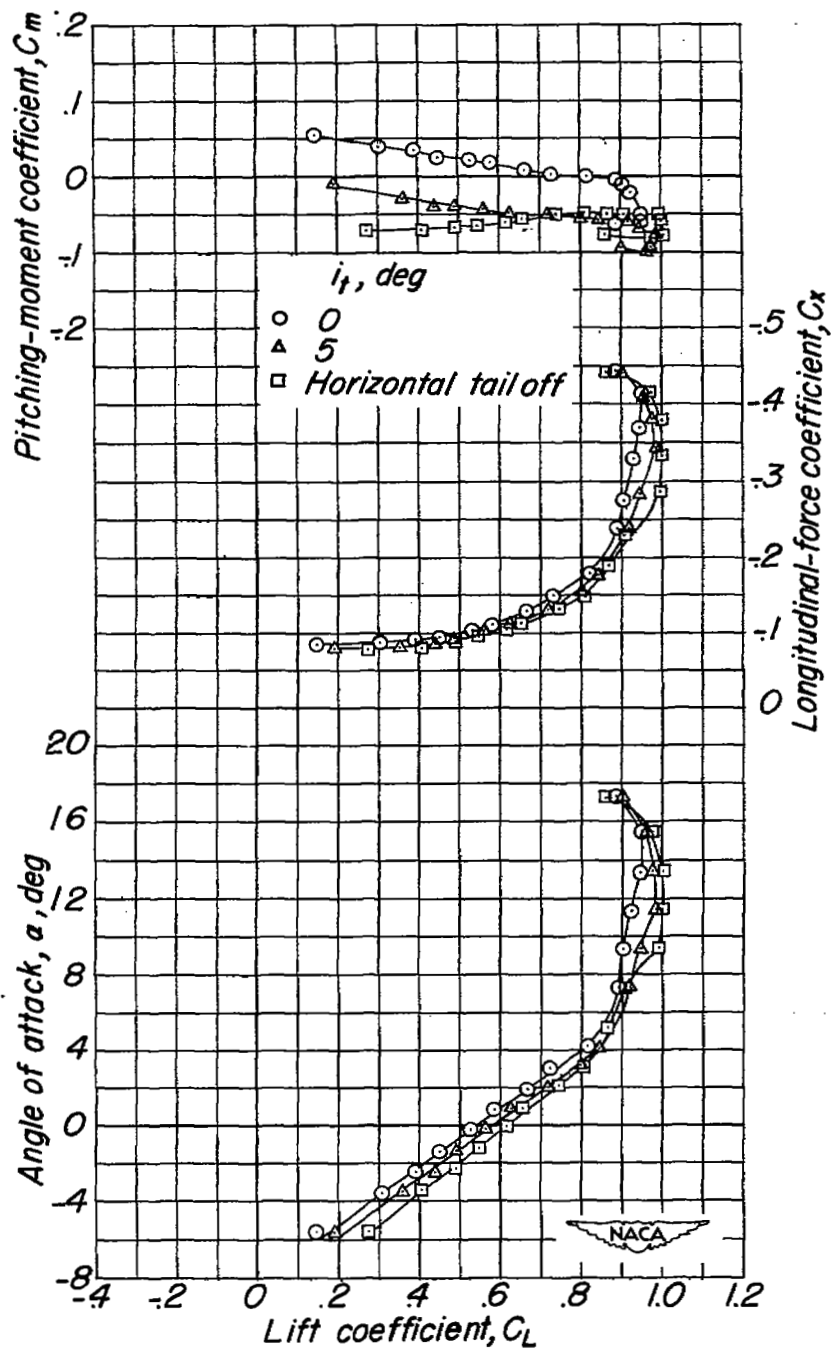
(e) Inboard-end chord-extension location, 65 percent wing semispan; chord-extension span, 20 percent wing semispan; overhang,  $0.10c$ .

Figure 14.- Concluded.



(a) Clean-wing model.

Figure 15.- The effect of the tail on the aerodynamic characteristics of the test model.  $\delta_T = 50^\circ$ ;  $\delta_{n_1} = 0^\circ$ ;  $\delta_{n_2} = 0^\circ$ ;  $\delta_{n_3} = 0^\circ$ .



(b) Inboard-end of chord-extension location, 65 percent wing semispan; chord-extension span, 20 percent wing semispan; overhang, 0.15c.

Figure 15.- Concluded.

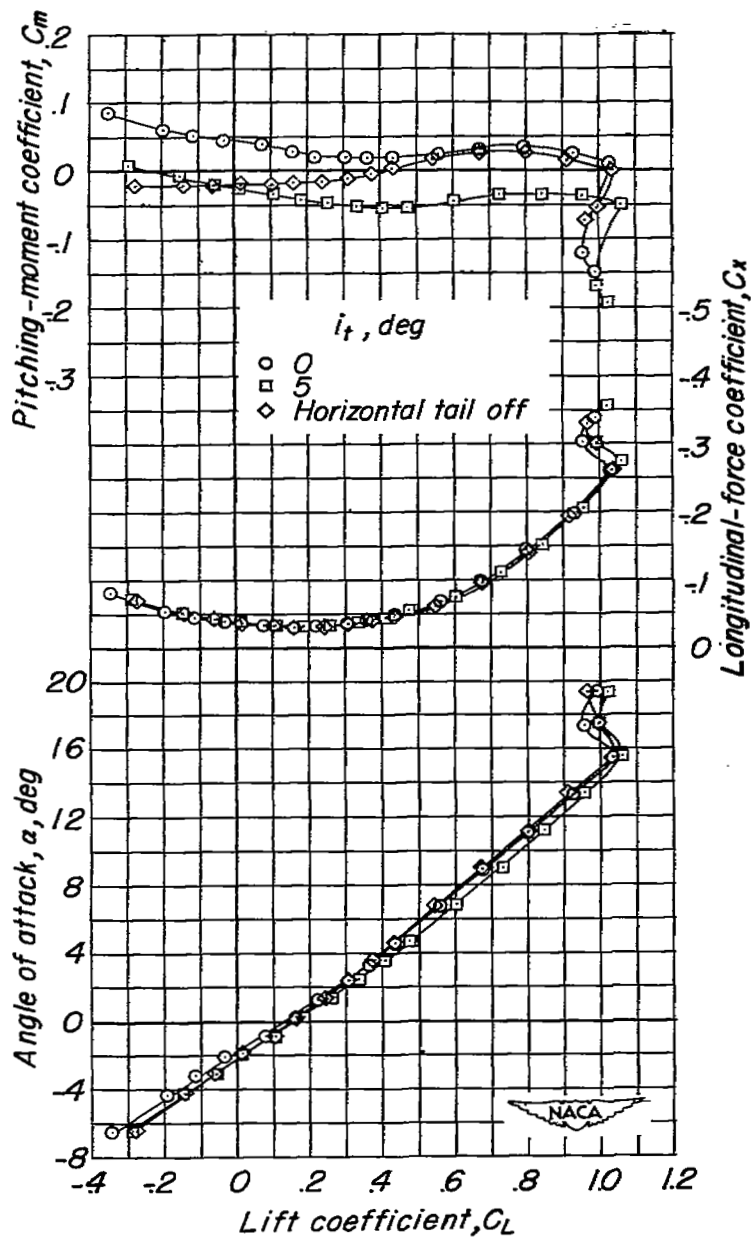
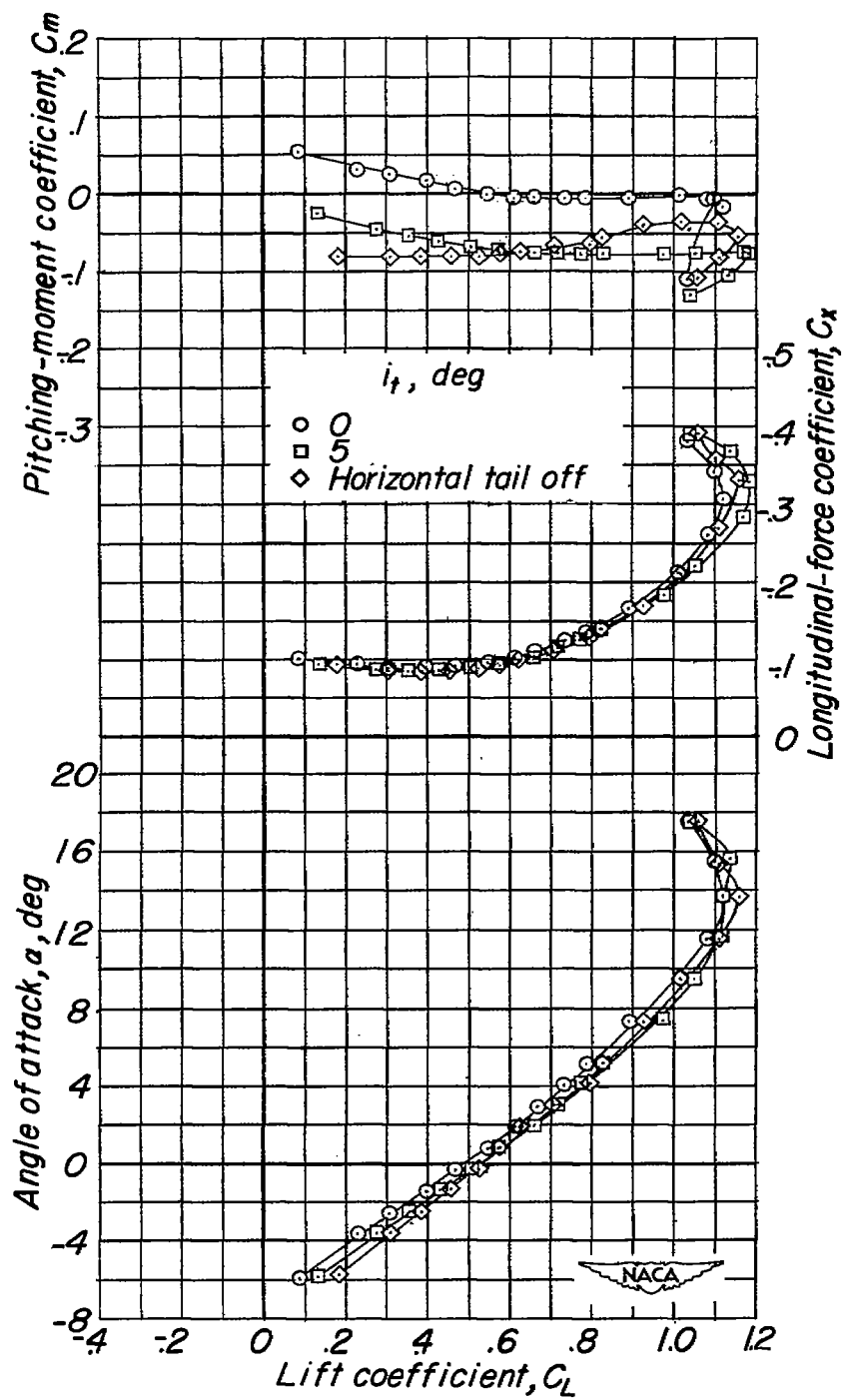
(a)  $\delta_f = 0^\circ$ .

Figure 16.- The effect of the tail on the aerodynamic characteristics of the test model incorporating wing leading-edge deflection in conjunction with a chord-extension. Chord-extension span extends from  $0.65b/2$  to wing tip; overhang,  $0.15c$ ;  $\delta_{n_1} = 0^\circ$ ;  $\delta_{n_2} = 18^\circ$ ;  $\delta_{n_3} = 18^\circ$ .



(b)  $\delta_F = 50^\circ$ .

Figure 16.- Concluded.

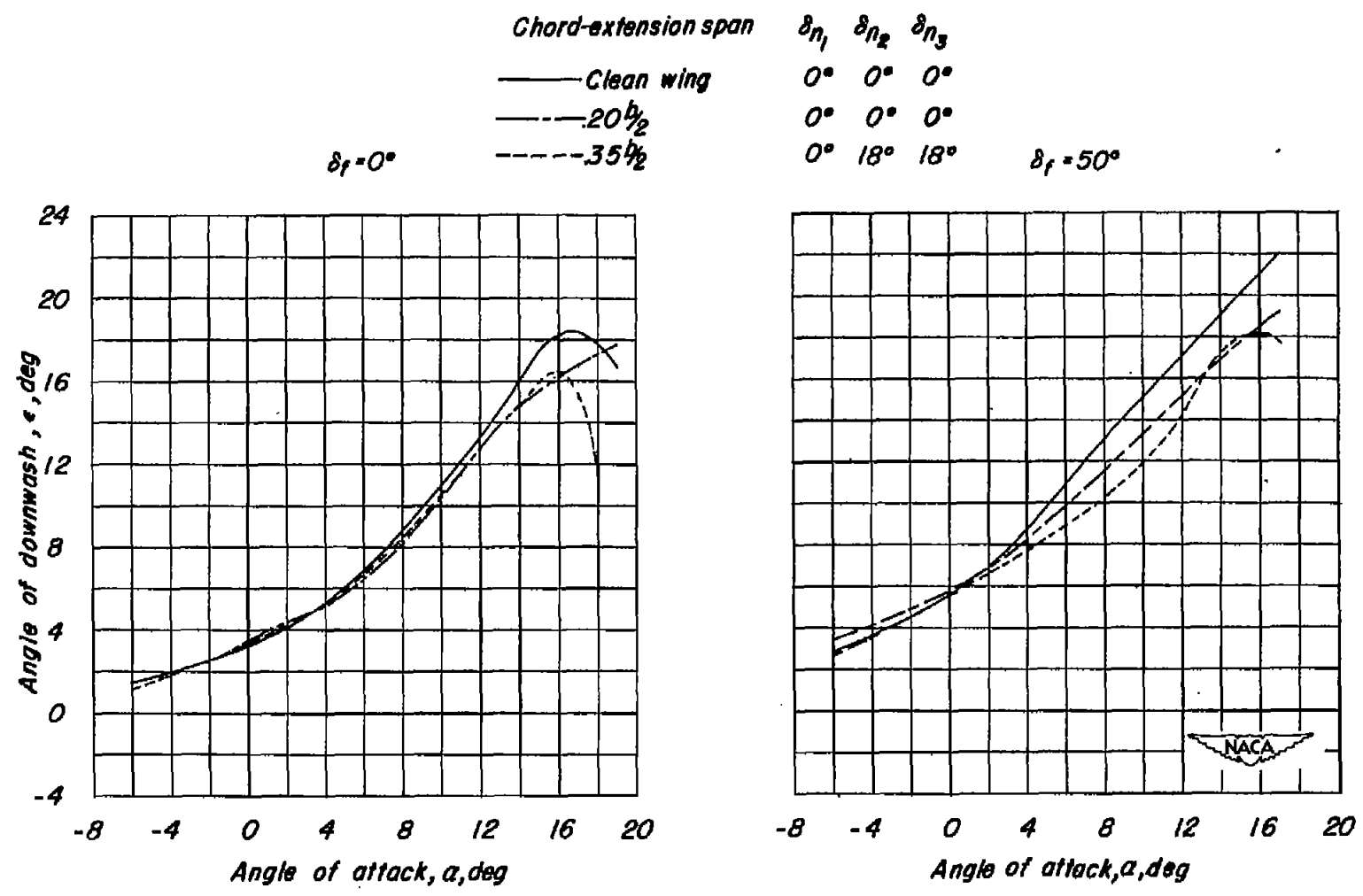


Figure 17.- The effect of chord-extensions on the effective downwash characteristics at the tail of the test model. Chord-extension inboard-end location,  $0.65\frac{b}{2}$ ; overhang,  $0.15c$ .

Chord-extension span	$\delta_{n_1}$	$\delta_{n_2}$	$\delta_{n_3}$
— Clean wing	0°	0°	0°
- - .20 $\frac{b}{2}$	0°	0°	0°
- - - .35 $\frac{b}{2}$	0	18°	18°

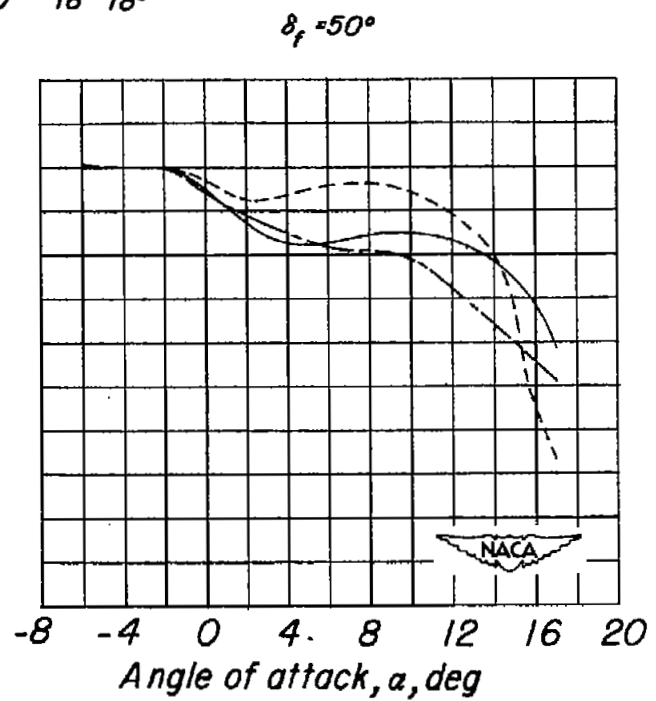
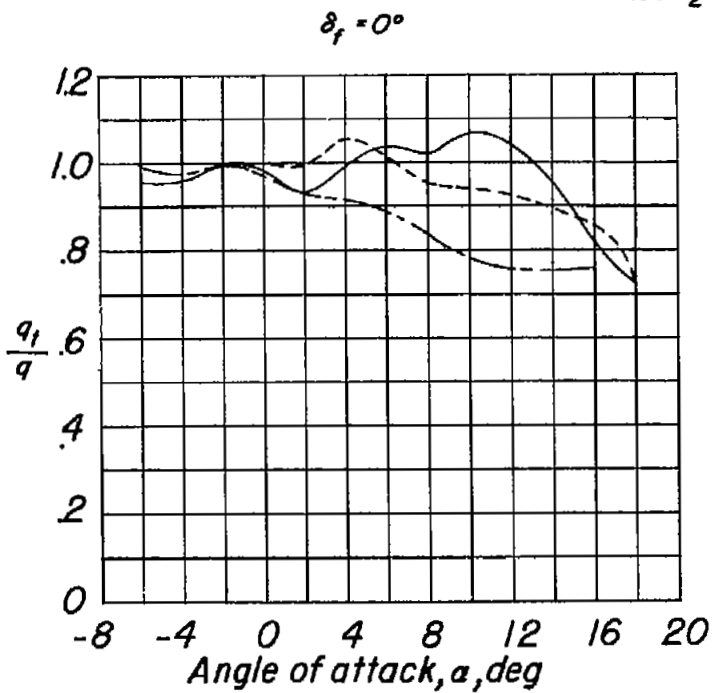


Figure 18.- The effect of chord-extensions on the dynamic pressure at the tail of the test model. Chord-extension inboard-end location,  $0.65b/2$ ; overhang,  $0.15c$ .

Chord-extension span	$\delta n_1$	$\delta n_2$	$\delta n_3$
— Clean wing	$0^\circ$	$0^\circ$	$0^\circ$
- - - $.20b/2$	$0^\circ$	$0^\circ$	$0^\circ$
- - - $.35b/2$	$0^\circ$	$18^\circ$	$18^\circ$

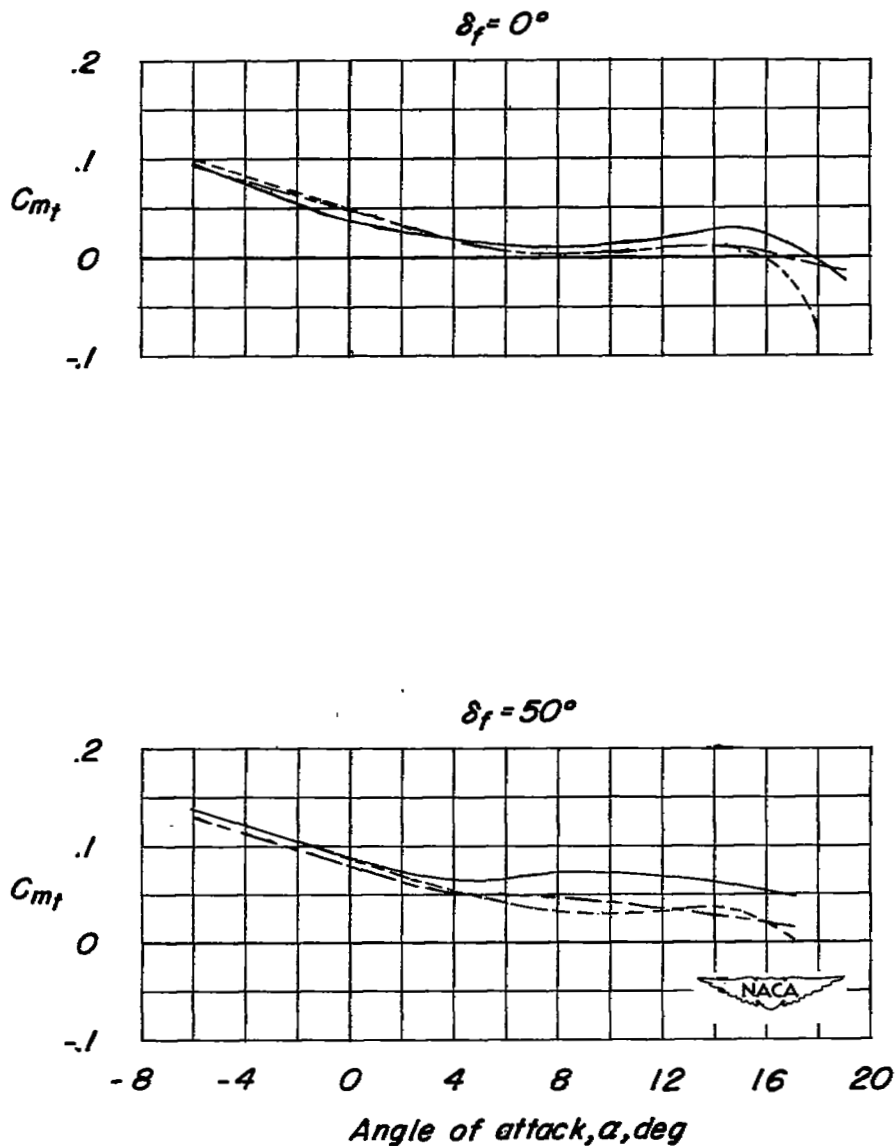
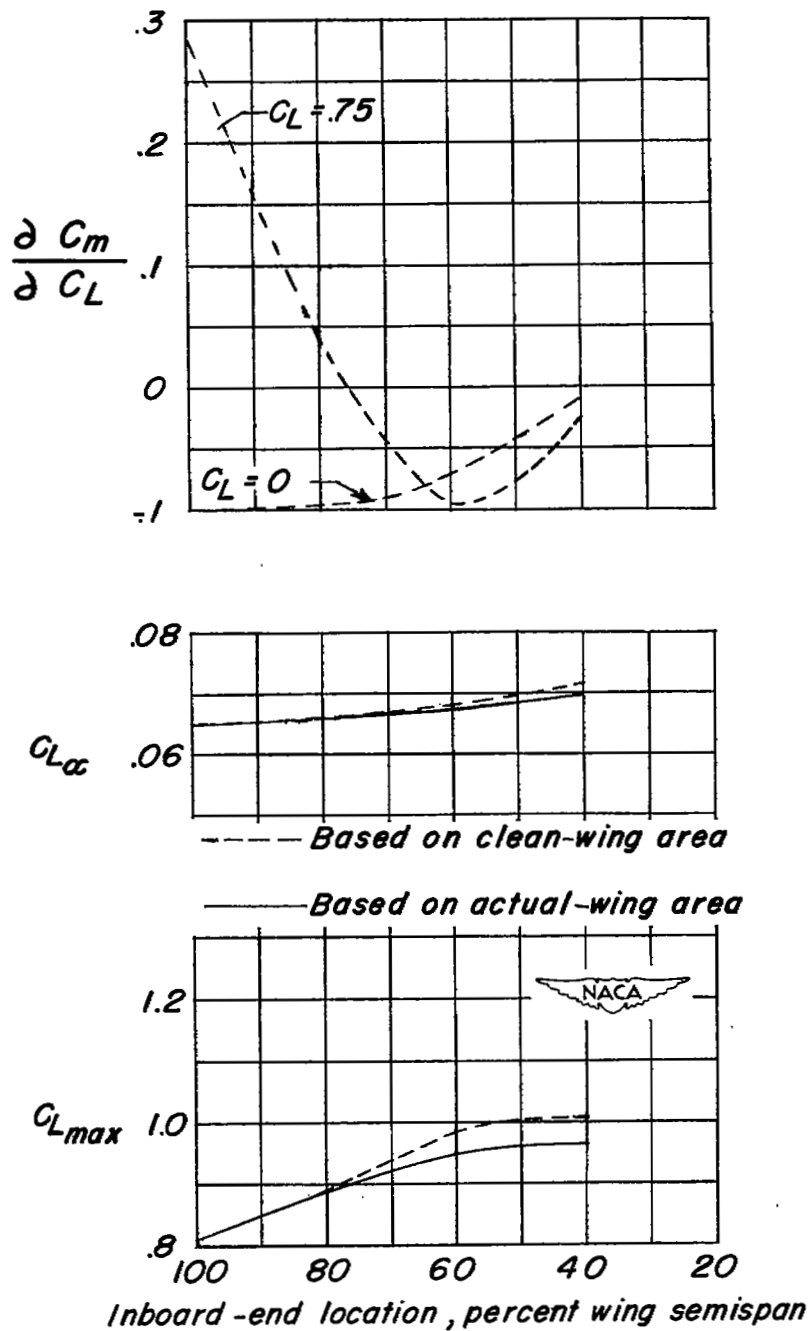


Figure 19.- Tail contribution to the pitching-moment characteristics of the test model,  $i_t = 0^\circ$ . Chord-extension inboard-end location,  $0.65b/2$ ; overhang,  $0.15c$ .



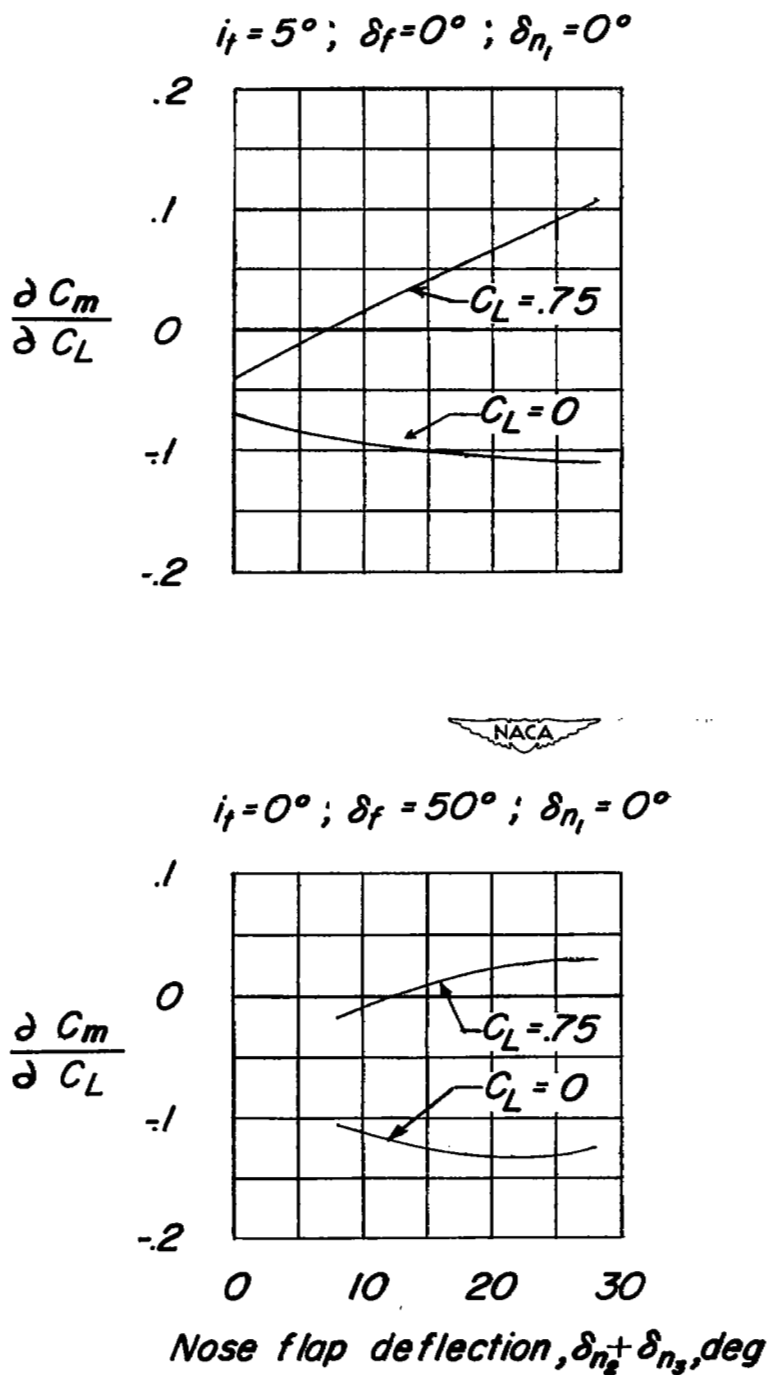
- (a) Chord-extension overhang,  $0.15c$ ;  $i_t = 0^\circ$ ;  $\delta_f = 0^\circ$ ;  $\delta_{n1} = 0^\circ$ ;  
 $\delta_{n2} = 0^\circ$ ;  $\delta_{n3} = 0^\circ$ ; outboard end fixed at wing tip.

Figure 20.- Summary of aerodynamic characteristics for the test model.

# ***Error***

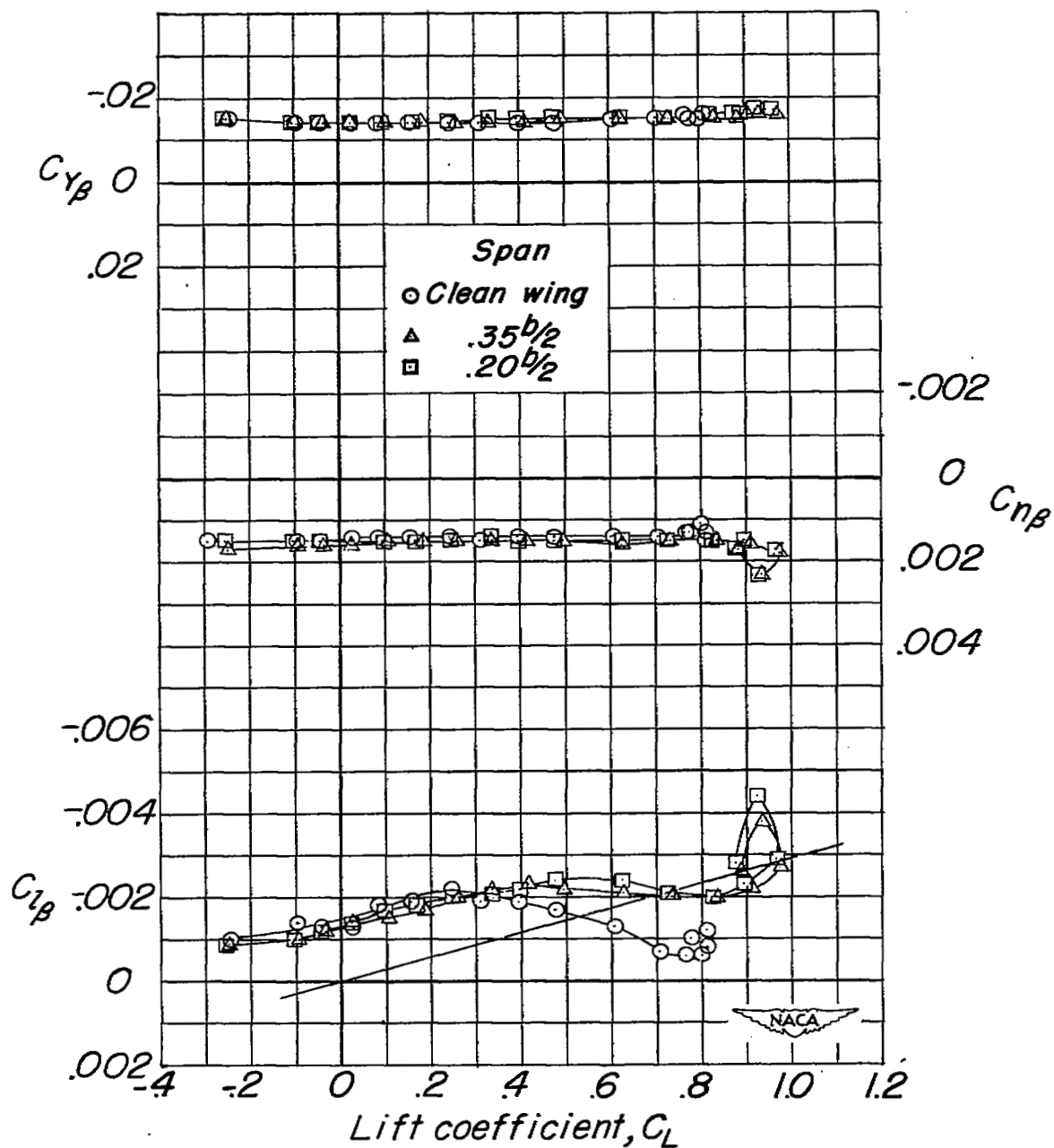
---

An error occurred while processing this page. See the system log for more details.



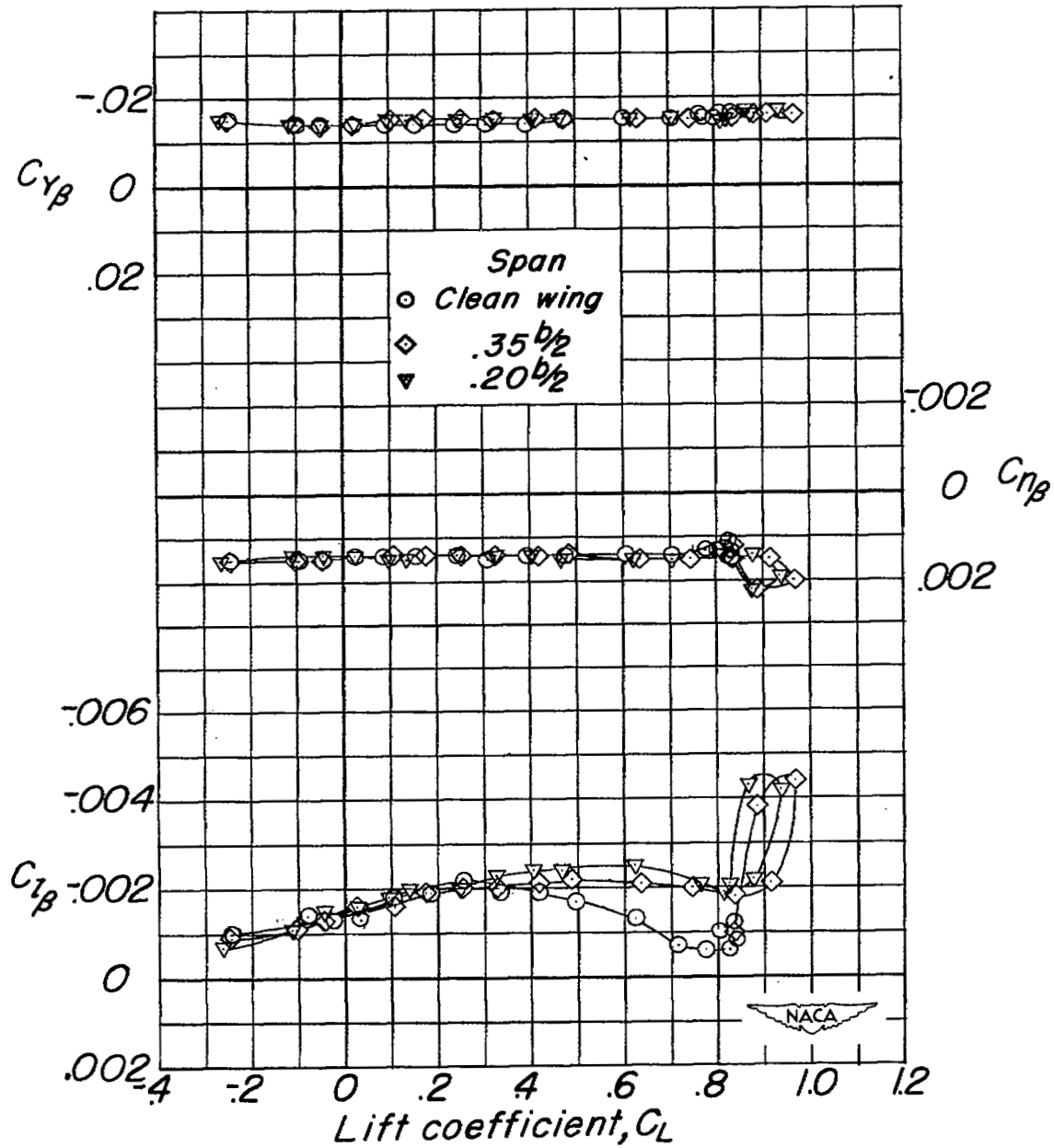
(c) Chord-extension overhang,  $0.15c$ ; inboard end of chord extension located 65-percent wing semispan.

Figure 20.- Concluded.



(a) Chord-extension overhang, 0.15c.

Figure 21.- The effect of chord-extension span on the lateral-stability parameters of the test model. Inboard-end chord-extension located 65 percent wing semispan;  $i_t = 0^\circ$ ;  $\delta_f = 0^\circ$ ;  $\delta_{n1} = 0^\circ$ ;  $\delta_{n2} = 0^\circ$ ;  $\delta_{n3} = 0^\circ$ .



(b) Chord-extension overhang, 0.10c.

Figure 21.- Concluded.

SECURITY INFORMATION

NASA Technical Library



3 1176 01436 9475

